Faculty of Natural Science and Technology
Department of Physics

NTNU
Innovation and Creativity

MASTER'S THESIS FOR

STUD. TECHN. INGRID LANGDAL

Thesis started:	20.01.2009
Thesis submitted:	16.06.2009

DISCIPLINE: MEDICAL PHYSICS

English title: *"Dosimetry and evaluation of algorithm for inverse optimized doseplanning for brachytherapy"*

Norsk tittel: *"Dosimetri og vurdering av algoritme for invers optimalisert doseplanlegging for brachyterapi"*

This work has been carried out at St. Olavs Hospital, under the supervision of Anne Dybdahl Wanderås

---

Trondheim, 16.06.2009

Tore Lindmo

Responsible supervisor

Professor at Department of Physics

Preface

This report is written by Ingrid Langdal, student at biophysics and medical technology at the Norwegian University of Science and Technology. This work is done during the tenth semester, and counts for 30 points.

In this study, a new treatment planning algorithm for brachytherapy have been tested, and the possibility to take this algorithm in use at St. Olavs Hospital have been evaluated. This study is performed in collaboration with St. Olavs Hospital.

This study is a continuation of my project work done fall 2008. Most parts of chapter 2.1 and 3.1 are similar to that written in the project work, but is considered necessary to include in this work for completeness. The evaluation method used for the treatment plans is as suggested in the project work [1].

I would like to thank my teaching supervisor at St. Olavs Hospital, medical physicist at the Department of Oncology, Anne Dybdahl Wanderås, for initiation and continous follow-up throughout the execution of this study. My internal supervisor at the university was professor Tore Lindmo, and for that I would like to thank him.

I would also like to give thanks to Anne Beate Langeland Marthinsen for guidance when writing the report, Signe Danielsen for informative contribution, Thorbjørn Tveit for creating a data base that systemized and calculated all values of interest and Marit Sundseth, the physician responsible for treatment of the patients included in this study.

Abstract

Purpose

Individual optimized treatment planning is recommended when creating treatment plans for brachytherapy of cervical cancer. Manual alteration of the dose distribution is time consuming and the treatment plan may be dependent on the person creating it. Inverse planning simulated annealing (IPSA) is an algorithm that can optimize the dose distribution considering dose to several delineated stuctures. This algorithm, currently available in the treatment planning system Masterplan, has been evaluated for brachytherapy of cervical cancer.

The Masterplan system simulates a source type from at different manufacturer than the type used for treatment at St. Olavs Hospital at the time being. The dose distribution from the two source types were evaluated to see if Masterplan can be used to simulate the source type used for treatment at St. Olavs Hospital.

Methods and materials

The dose distributions from the two source types were compared based on calculations from two treatment planning systems (Masterplan and Plato) simulating each source type.

Dose measurements of the source used at St. Olavs Hospital for brachytherapy treatment of cervical cancer were taken. These were compared with the dose distribution calculated by the two treatment planning systems.

At St. Olavs Hospital treatment are executed using a Fletcher type applicator. MR-images are taken with the applicator in place. Target and organs at risk are delineated in the images before the treatment planning is performed. For 11 patients treated with brachytherapy of cervical cancer at St. Olavs Hospital, three different IPSA-plans with different dose constraints (ISPA1, IPSA2 and IPSA3) and one treatment plan with equal dwell times were made in retrospect. All IPSA-plans constrain the same dose to the target. IPSA1 and IPSA3 have the same constraints to organs at risk, while IPSA2 allow a higher dose to the organs at risk. IPSA3 sets a limit for maximum dose in target volume. For evaluation of the quality of the treatment plans, dose parameters of clinical relevance were extracted from dose volume histograms.

Results

Deviations in the calculated dose distribution up to 30% is found for the two source types in certain areas. These deviations are found close to the source and below the connector end of the source. For distances ≥ 4 mm from the source center along one axis, deviations of the calculations were $\leq 4\%$. This is in correspondance with the measured dose values.

Target coverage for IPSA2 is 0.92. For ISPA1 and IPSA3 target coverage is 0.84 and 0.81 respectively. The number of treatment plans exceeding tolerance limit for one or more OAR is 82% for IPSA2, 55% for IPSA1 and 35% for IPSA3. The plan

with equal dwell times have a target coverage of 0.66 and 45% of the treatment plans exceed the given tolerance limit for one or more organs at risk.

Conclusion

Deviations are found in the simulated dose distribution of the two source types tested, but only in clinical irrelevant areas for brachytherapy of cervical cancer. Masterplan can be used for simulating the dose distribution of the source used for treatment at St. Olavs Hospital.

Using IPSA is better when it comes to improving target coverage and not violating tolerance limit for organs at risk, than a conservative treatment plan with equal dwell times. Due to too high doses to organs at risk, IPSA2 should be rejected. IPSA1 has better target coverage and IPSA3 have lower dose to the organs at risk. To avoid inhomogeneities in dwell time values, ISPA3 is probably the best suggestion.

Sammendrag

Formål

Det er anbefalt å lage individuelt optimaliserte planer når behandlingsplaner skal lages i forbindelse med brachyterapi av livmorhalskreft. Manuell endring av dosefordelingen er tidkrevende og resultatet kan bli preget av personen som lager planen. 'Iverse planning simulated annealing' (IPSA) er en algoritme som kan optimalisere dosefordelingen slik at dose til flere skisserte strukturer blir tatt hensyn til. Denne algoritmen, tilgjengelig i doseplanleggingssystemet Masterplan, har blitt vurdert for brachyterapi av livmorhalskreft.

Masterplan simulerer en kildetype fra en annen produsent enn den kildetypen som blir brukt til behandling på St. Olavs hospital i dag. Dosefordelingen til de to kildetypene har blitt vurdert for å se om Masterplan kan brukes til å simulere kildetypen brukt til behandling.

Metode og utstyr

Dosefordelingen fra de to kildetypene ble sammenlignet ved hjelp av doseberegninger fra to doseplanleggingssystemer (Masterplan og Plato) som simulerer hver sin kildetype.

Det ble tatt målinger av dosen fra kilden brukt på St. Olavs hospital til brachyterapi av livmorhalskreft. Disse ble sammenlignet med dosefordelingen regnet ut av de to planleggingssystemene.

På St. Olavs hospital blir en Fletcher type applikator brukt til behandling. MR-bilder blir tatt etter at applikatoren er posisjonert. I bildene blir målvolum og risikooganer skissert før behandlingsplanleggingen gjennomføres. I denne studien har tre ulike IPSA-planer med forskjellig doserestriksjoner (ISPA1, IPSA2 and IPSA3) og en plan med lik liggetid i kildeposisjonene, blitt laget i ettertid for 11 pasienter behandlet for livmorhalskreft på St. Olavs hospital. ISPA-planene har samme doserestriksjoner til målvolum. IPSA1 og IPSA3 har samme begrensning til risikoorganer, mens IPSA2 tillater høyere dose til risikoorganer. IPSA3 har en begrensning for maksimum dose til volum for målvolumet. For vurdering av kvaliteten til planene ble klinisk relevante doseparametre funnet fra dosevolum-histogram.

Resultat

Det ble funnet avvik opp til 30% for beregnet dose i ulike punkt for de to kildetypene i visse områder. Disse avvikene ligger nærme kilden og rett under koblingsenden. For avstander ≥ 4 mm fra kildesenter transversalt på kilden er avvikene i beregningene $\leq 4\%$. Dosemålingene som ble tatt støtter dette.

Dekning av målvolum er 0.92 for IPSA2. For IPSA1 og IPSA3 er denne dekningen henholdsvis 0.84 og 0.81. Antall planer hvor en definert grense for dosen til et eller flere risikoorgan har blitt oversteget, er 82% for IPSA2, 55% for IPSA1 og 35% for IPSA3. Planen hvor liggetidene er fordelt likt har målvolumdekning på

0.66 og 45% av planene overstiger den definerte toleranse grensen for et eller flere risikoorgan.

Konklusjon

Det ble funnet avvik i de simulerte dosefordelingene mellom de to kildetypene, men kun i klinisk irrelevante områder for brachyterapi av livmorhalskreft. Masterplan kan bli brukt til å simulere dosefordelingen til kilden som blir brukt til behandling på St. Olavs hospital.

Bruk av IPSA gir bedre resultater enn den konservative behandlingsplanen med lik liggetid når det gjelder dekning av målvolum og å overholde toleransegrensene som er satt for risikorganene. På grunn av for høye doser til risikoorganer burde IPSA2 forkastes. IPSA1 gir bedre dekning av målvolum mens IPSA3 gir lavere dose til risikoorganer. For å unngå store forskjeller mellom liggetidene i de ulike kildeposisjonene vil antagelig IPSA3 gi best utganspunkt for videre planlegging.

Contents

Abbreviations

KERMA $\frac{dE_{tr}}{dm}$ - The sum of the initial kinetic energy of all charged ionizing particles released in a material, dm. (Gy)

Air KERMA rate Kerma to air, in air, at 1 m reference distance, corrected for scatter and attenuation (μGy/h)

CTV Clinical target volume

OAR Organ at risk

Normal tissue All body tissue not defined as target or OAR

CTV D90 The minimum dose in 90% of the target volume (Gy)

CTV V100 The target volume receiving the prescribed dose (cm^3)

CTV V400 The target volume receiving 400% of the prescribed dose (cm^3)

EXT V100 The volume of normal tissue receiving the prescribed dose (cm^3)

OAR$_{D2\,cm^3}$ The minimum dose in the 2 cm^3 volume receiving the highest dose of the given OAR (Gy)

IPSA Inverse planning simulated annealing

EDT Plan with equal dwell times

DVH Dose volume histogram

1 Introduction

The ninth most common type of cancer in Norway is cervical cancer. The incidence of cervical cancer has been decreasing over the last 40 years, mostly due to systematic screening of all women between 25 and 69. Every year 270 new incidences of cervical cancer occur (2004). The lethality is 0.37. Half of the women where cervical cancer is demonstrated have never taken the cell test in the screening routine, and the cancer stage is often advanced [2].

While early stage cervical cancer is usually treated surgically, locally advanced cervical cancer is treated with intracavitary brachytherapy in combination with external radiotherapy and chemotherapy. The aim of radiotherapy is to give high doses to tumor tissue, while sparing the adjacent normal tissue. Functionality of nearby organs may be reduced or damaged if the organs receive too high doses.

Traditionally there were little information available of a patient's individual anatomy when creating a treatment plan for intracavitary brachytherapy. Therefore standard treatment plans were used. The radiation dose was prescribed to a geometrical point A considered to be representative for the minimum dose to most malignant tissue [3]. 3D imaging techniques have now become available, and with the information from these images it is possible to create individually optimized treatment plans.

From international recommendations, treatment planning of cervical cancer should be based on individual anatomy [4]. Several hospitals, including St. Olavs Hospital, have started using individually optimized treatment plans. Treatment plans are manually altered to get the desired dose distribution, i.e. an optimized treatment plan. This is time consuming. To save time and to make the treatment planning less subjective, an inverse planning simulated annealing (IPSA) algorithm has been suggested. This algorithm is currently available in the treatment planning system Masterplan.

IPSA imports dose constraints set by the radiotherapist, and finds the best possible solution matching these constraints. Different constraints can be specified [5]. In the present study, three different sets of dose constraints have been tested. The IPSA-optimized treatment plans are also compared to a more conservative treatment plan.

This is a retrospective study where four different treatment plans have been made for patients that previously have been treated at St. Olavs Hospital.

The IPSA module currently available in Masterplan, simulates a source type from a different manufacturer than the one used at St. Olavs Hospital. The geometries of these two source types are slightly different [6], and therefore it is important to examine if and how the dose distribution around the two source types differ and how this clinically affect the brachytherapy treatment of cervical cancer.

2 Theory

2.1 Brachytherapy of cervical cancer

2.1.1 Brachytherapy

Brachytherapy is a form of radiation therapy where a radioactive source is placed within or in close proximity to the volume requiring treatment. For intracavitary brachytherapy (ICBT) the source is placed in body cavities, and a common application of ICBT is treatment of cervical cancer.

In brachytherapy the dose fall-off around the radioactive source is rapid. This makes it possible to deliver a high dose to the tumor volume, while at the same time reduce the dose to the surrounding tissue. Different dose rates can be used; low dose rate (LDR), medium dose rate (MDR) and high dose rate (HDR). If the dose rate delivered is high (HDR: $\geq$ 12 Gy/h), the treatment time is short (ca $5 - 15$ min) and the number of fractions are limited. Short overall treatment time reduces the risk of tumor repopulation [3].

Different radioactive sources can be used for ICBT. At St. Olavs Hospital the equipment is adapted to ^{192}Iridium, a commonly used source for ICBT. This is a γ-emitter, as most sources used in brachytherapy (β-emitting sources are more common for shallow lesions). One of the reasons for using ^{192}Iridium is the high specific activity (activity per unit mass of a radionuclide). This gives a high dose rate, and also helps miniaturization of brachytherapy sources [3].

2.1.2 Cervical cancer

The uterus is situated in the central part of the pelvis, between the bladder and the rectum. The lower part of the uterus is called cervix uteri. Most incidences of cervical cancer have its origin from the mucous membrane between the outer part of the cervix and the vagina, see figure 1 [2].

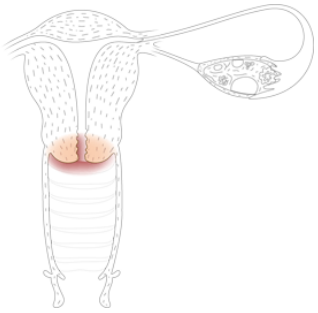

Figure 1: *Illustration of the region where most incidences of cervical cancer have its origin. The vagina is shown in the bottom part of the picture, the upper part shows the uterus. One ovary is drawn to the right* [2].

Early stage cervical cancer is usually treated surgically. Exceptions are made by risk of complications because of comorbidity. Locally advanced cervical cancer

is treated with chemoradiation. At St. Olavs Hospital the standard treatment is external radiation treatment combined with weekly Cisplatin and brachytherapy, where ICBT plays a very important role in the attempt to cure the patient. This treatment is chosen whenever surgery alone is unlikely to cure the patient [7][8].

2.1.3 Target volumes in brachytherapy of cervical cancer

The Groupe Europeen de Curietherapie - European Society for Therapeutic Radiology and Oncology (GEC-ESTRO) working group has made recommendations on how to delineate target volumes on digital images in brachytherapy of cervical cancer [4]. The gross tumor volume, GTV, should include the gross demonstrable extent and location of the malignant growth. The clinical target volume, CTV, is defined as the volume containing both GTV and subclinical microscopic malignant disease [9]. The CTV is divided into two subvolumes for radiotherapy planning purposes. *High risk* CTV (HR CTV) includes GTV, the whole cervix and the presumed extracervical tumor extension. No safety margins are added. *Intermediate risk* CTV (IR CTV) encompasses high risk CTV with safety margin of $5 - 15$ mm. Safety margin is chosen according to tumor size and location, potential tumor spread, tumor regression and treatment strategy. Examples of the delineated volumes are shown in figure 2. All tissue included in CTV should be neutralized in order to cure the patient [3].

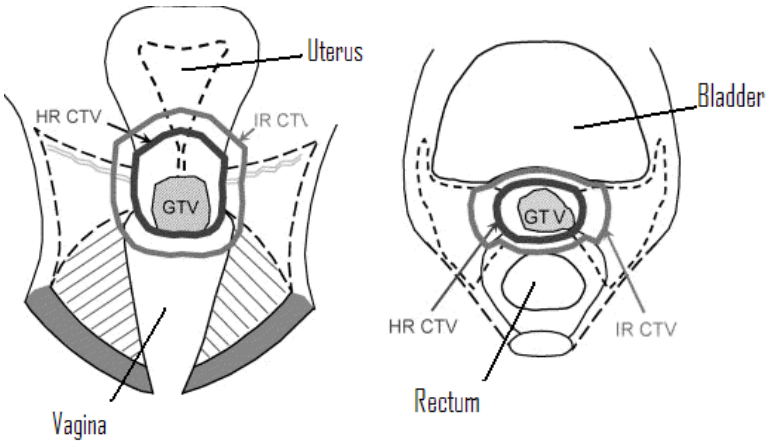

(a) Frontal plane (b) Transversal plane

Figure 2: *Illustration of* GTV *and* CTV *in brachytherapy treatment of cervical cancer* [4].

2.1.4 Applicators

To perform brachytherapy treatment of cervical cancer an applicator is inserted into the uterus and inner part of vagina. The applicator is connected to a remote afterloader, which loads the source into the applicator for treatment. The

afterloader system applied in this study uses a stepping source, i.e. one source is placed in different positions in the applicator for a certain amount of time to give the desired dose distribution [3].

Two different types of applicators are widely used for brachytherapy of cervical cancer, namely Fletcher type and ring type. Both consist of a central uterine applicator that is positioned in the uterus. In addition to this, the Fletcher applicator have two ovoid applicators and the ring type has a ring applicator, both placed in the inner part of the vagina close to the cervix. Both of the applicator types have the possibility to geometrically fit to different anatomical structures and pathological situations for the individual patient. The two different applicator types are shown in figure 3.

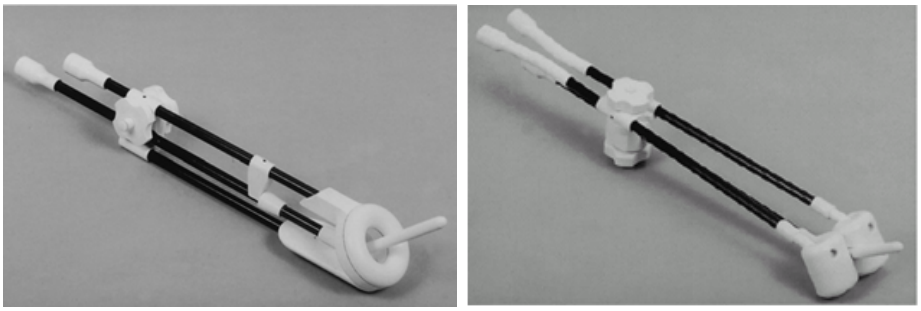

(a) Ring type (b) Fletcher type

Figure 3: *Ring and Fletcher type applicators.*

At St. Olavs Hospital a Fletcher type applicator is used. This applicator was developed by Fletcher, who made a system for radium that consists of a rigid metallic intrauterine applicator and two ovoid applicators. Subsequently this system was modified, first for manual afterloading, and later also for remote afterloading. It has also been adapted to the use of different sources [3]. The Fletcher type used at St. Olavs Hospital is shown in figure 4.

Figure 4: *The Fletcher type applicator used at St. Olavs Hospital* [10].

2.1.5 Treatment techniques

Different traditions for treatment techniques of brachytherapy of cervical cancer exist. These different systems are sets of rules based on applicator type, geometry and source intensity, in order to give the best dose distribution in the target volume.

The three main systems are the Stockholm-, Paris- and Manchester system [3]. The Stockholm system is based on a ring applicator, the Paris system is based on a 'mould' individual shaped applicator while the Manchester system is based on an applicator consisting of an uterine- and to ovoid applicators.

Traditionally the Fletcher and ring applicators have been used with standard treatment plans. The standard treatment plan formerly used at St. Olavs Hospital was developed from the Manchester system, where the dose was prescribed to a so-called point A. Point A was considered to be representative for the minimum dose to most of the malignant tissue and is defined from the geometry of the applicator. A plan made on the basis of dose to point A does not take into consideration the variation of the anatomy between different patients.

With 3D-image techniques available today it is possible to make individual treatment plans for every patient. Target volume and organs at risk (OARs) can be delineated from CT or MR-images, and then it is possible to create a treatment plan with best possible fitting of isodose lines to the target volume, and at the same time give acceptable doses to the OARs. GEC-ESTRO working group has recommended that target volume should be the basis of dose distribution, and not the dose to point A [4].

Fitting the isodose lines to the target volume and the organs at risk are usually done manually in a treatment planning system. Recently new computer programs have become available for inverse optimization planning, where the program can consider both target volume and the dose to other delineated structures.

2.1.6 Organs at risk

The use of radiation therapy inevitably involves exposure to the surrounding normal tissue. Some healthy tissue tolerates curative radiation doses rather well, while for other organs the consequences of irradiation are severe. The dose must then be tailored to minimize the likelihood of serious injury. The pathological process of radiation injury begins immediately after radiation exposure, but the clinical outcome may not become apparent for weeks, months or years later [11]. When symptoms appear during treatment or within a few weeks after, the effect is defined as acute. This effect is most prominent in tissue with rapidly proliferating cells. Late effects come from tissue with a slow turnover, and the symptoms might not emerge before months or years after treatment. The effects on the surrounding tissue are dependent on total dose, dose per fraction and fractionation rate [12].

When radiation therapy is performed in a certain region, a number of local organs can be specified as OARs. These organs are either in close proximity to the tumor or they are radiosensitive and this will influence the treatment planning.

Damage to one of these organs may reduce the quality of life of the patient, and keeping doses under the tolerance limits for these organs are of great importance during treatment planning. For radiation of cervical cancer these specified OARs are bladder, rectum and sigmoid [3][13].

The tolerance dose of the OAR depends upon the organs functional reserve and structural organization. Organs are often divided into two groups physiologically; parallel-like and serial-like. This is analogous to an electrical circuit, where a shunt circuit will still function after damage in one part of the circuit, but a serial connection will not. Parallel like organs are for example kidney and liver, and damage to parts of these organs will only lower the functionality, not fully damage the organ. A typical serial like organ is the spinal cord, were a patient can be paralyzed after damage to only a small fraction of the organ. Bladder, rectum and sigmoid are all serial like organs, where damage to parts of this organ can damage the functionality by for instance making a hole in the organ wall [9].

Due to this fact, small organ volumes irradiated with the tolerance dose or higher, is of greater interest than the average dose to the entire volume of the organ when assessing late effects of OARs from brachytherapy of cervical cancer. In addition to this, the dose delivered to the typical OARs from brachytherapy is inhomogeneous, unlike what is assumed for external beam radiation therapy. The part of the organs that is situated adjacent to the radiation source will receive a much higher dose than the parts further away. This is visualized in figure 5.

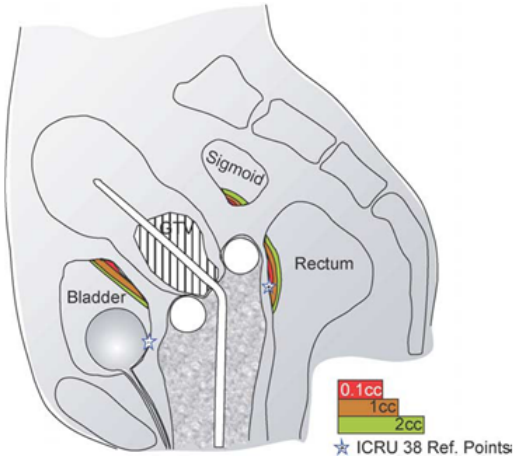

Figure 5: *Schematic anatomical diagram indicating the most irradiated tissue volumes in* OARs *(0.1, 1 and 2* cm^3*) in brachytherapy of cervical cancer* [13].

There is also a general agreement that correlating point doses and dose volume effects is insufficient, since damage to a point is not of clinical relevance. The dose will not be of clinical relevance until a certain size of the OAR reaches a tolerance level. For bladder, rectum and sigmoid this critical size is correlated with the thickness of the organ wall, and if this volume is irradiated with more than the tolerance dose, there is a large probability for damaging the function of the OAR.

Therefore it is recommended to indicate the lowest dose to the limited volume of the OAR that receives the highest dose. This bear clinical relevance. Regarding bladder, rectum and sigmoid, a volume of 2 cm^3 is recommended. Dose to this volume should correlate to side effects [13].

The OARs are presumed to have a given tolerance dose for the total treatment, external and internal radiotherapy. The minimum dose in the 2 cm^3-volume receiving the highest dose of the OAR, should not exceed this tolerance limit. From recommendations from R. Pötter [14], the limit for the bladder is 90 Gy and for rectum and sigmoid it is 75 Gy. These limits are calculated into biological doses relative to 2 Gy fractions (equation (1)).

2.1.7 Biological equivalent dose

Biological equivalent dose after different radiation regimen can be calculated by means of the linear quadratic model. Here, biological dose of each fraction can be recalculated to show similar effect as if the dose is given in 2 Gy fractions. Since brachytherapy often is given with fraction doses $\geq$ 2 Gy, these doses need to be calculated into 2 Gy fractions. This is done by using equation (1), where EQD_2 is the biologically equivalent dose given with fraction dose of 2 Gy.

$$EQD_2 = nd \cdot \frac{d + \frac{\alpha}{\beta}}{2 + \frac{\alpha}{\beta}} \tag{1}$$

In equation (1) n is the number of fractions, d is the dose per fraction and α/β-ratio is the dose at which the linear (α) and quadratic (β) components of cell killing are equal from the linear-quadratic model [12]. This formula is used to calculate the total biologically weighted dose from all fractions, from both external and internal radiation therapy. For cervical cancer, GEC-ESTRO working group recommends to use $\alpha/\beta = 10$ for tumor tissue (early responding tissue), and $\alpha/\beta = 3$ for the OARs; bladder, rectum and sigmoid (late responding tissue) [13]. A higher α/β-value for bladder has also been suggested ($\alpha/\beta = 5 - 10$) [15], which will result in a lower equivalent dose converted into 2 Gy fractions if the fractionation is the same. Using $\alpha/\beta = 3$ gives a higher equivalent dose, and therefore, to be conservative, this value is chosen when converting to 2 Gy fractions [13].

2.2 Radiation dosimetry

2.2.1 Source types of interest

An aim of this work was to implement the brachymodule in the treatment planning system Masterplan in the routine at St. Olavs Hospital. The vendor of Masterplan does not support the source used for treatment at St. Olavs Hospital. Therefore an evaluation of the different source types was needed in order to see if the source type available in Masterplan can be used to simulate the treatment source. The source used for treatment at St. Olavs Hospital is specific for the GammaMed

12i HDR brachytherapy system. A source type available in Masterplan, Nucletron HDR classic, has similar geometry to the GammaMed source.

Both these source types are made of ^{192}Ir, which is one of the more stable radioisotopes of Iridium. The half life is 73.8 days, which is considerably longer than one fraction of brachytherapy, but replacement of the source is necessary every third month. The specific activity is high (9.2 Ci/g), making it suitable for brachytherapy making the treatment source able to fit into needles among other factors. The average photon energy is 380 keV.

GammaMed 12i HDR source This source type is used in GammaMed 12i HDR afterloader. It has an active length of 3.4 mm, active diameter of 0.6 mm, total diameter 1.1 mm and the distance from active end to tip is 0.86 mm. The encapsulation is stainless steel [6]. The GammaMed 12i HDR source is outlined in figure 6. Dosimetric evaluation of this source is presented in Ballester [16].

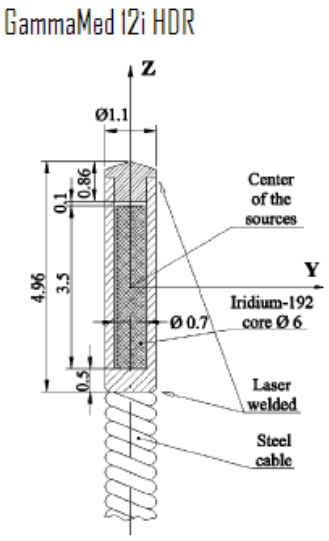

Figure 6: *Mechanical design of the GammaMed 12i* HDR *source. All dimensions are in* mm. [16].

Nucletron HDR classic This source type (figure 7) is used in the MicroSelectron HDR afterloader. The active length is 3.5 mm, active diameter 0.6 mm, total diameter 1.1 mm and the distance from active end to top is 0.35 mm. The encapsulation is stainless steel [6]. A dose rate table is presented in Williamson and Lie, among others [17].

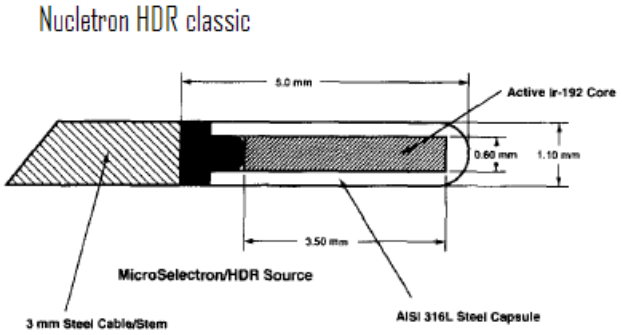

Figure 7: *Mechanical design of the Nucletron* HDR *classic source* [17].

The mechanical design of the GammaMed source is similar to the classic Nucletron source, except for a difference in distance from the active end to tip. This difference is 0.5 mm. The dose distribution from the Nucletron source and GammaMed source are compatible, with exceptions at angles less than 20° towards the steel cable end. Here the differences are said to range from 5-8%. The differences may be due to different densities in the cables [6].

According to Williamson and Li, the dose rate distribution reported for the Nucletron source should be applicable to the GammaMed source [17]. In Ballester they concluded that there was good agreement between the two dose distributions, except for points near the source. For these points the differences ranged from 5 to 25%. Differences were also found along the cable. Here the dose rate differences were up to 10% showing the influence of the cable [16].

2.2.2 Ionization chamber

An ionization chamber can be used for measuring the amount of ionizing radiation. The chamber is an instrument constructed to measure the number of ions, generated by the radiation, within a medium. It consists of a gasfilled enclosure with two electrodes between which a voltage is applied. The radiation interactions ionize the gas, and the electric field causes movement of the electric charges towards the electrode of opposite sign. This creates an accumulated charge that can be measured with an electrometer [18].

An ionization chamber is used to ensure that the dose delivered from a therapy unit is as intended. The chamber is connected to an electrometer that display the collected charge. A calibration factor is required converting the charge to dose rate.

Farmer chamber Multiple designs of ionization chambers have been developed for use in different situations. In this study a Farmer chamber was used for measuring the radiation dose from the GammeMed source. The Farmer chamber is a common design of cylindrical chamber for radiotherapy. The cylindrical outer wall acts as one of the electrodes and is made of graphite. The other electrode is a thin aluminum central rod. Most cylindrical chambers are supplied with a build-up cap, but this is not used when measuring in a phantom. These chambers can be used for both relative and absolute dose measurements, but for the latter case a calibration factor is necessary in order to determine the dose rate in absolute units at the reference point in water [18]. An illustration of the farmer chamber is shown in figure 8.

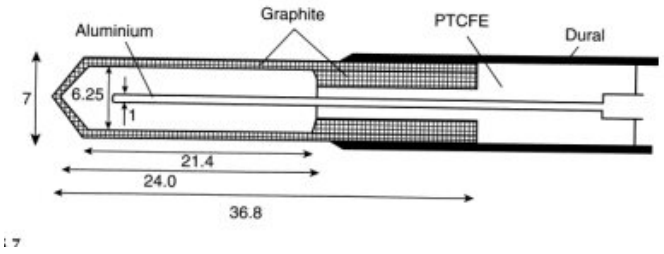

Figure 8: *An illustration of the farmer chamber. All dimensions are in* mm [18].

2.2.3 Electrometer

To measure the charge from the ionization chamber, an electrometer can be used. In most cases the electrometer includes a voltage supply and a display unit.

Most electrometers are based on negative-feedback operational amplifiers. The principle of such an electrometer is shown in figure 9. Negative feedback means that some or all of the amplifiers output is fed back to its negative input. Total feedback results in a gain of unity.

As seen in the figure, the negative input of the operational amplifier is connected to the chamber collection electrode and the positive input to a polarizing voltage or to the case ground. If then a capacitor or a resistor is connected in the feedback loop, the voltage measured at the output of the amplifier is proportional to the charge collected, and is equal to the voltage across the capacitor or resistor.

When a capacitor C is placed in the feedback loop and the voltage measured across the capacitor is V, then the charge collected, Q, is equal to CV. If instead a resistor R is placed in the loop, the voltage, V, measured across the resistor allows the current, I, to be determined as V/R [18].

2.2.4 Calculation from charge to dose rate in water

It was of interest to measure the dose from the source used at St. Olavs Hospital to see how well the measurements correlate with the similar calculated values

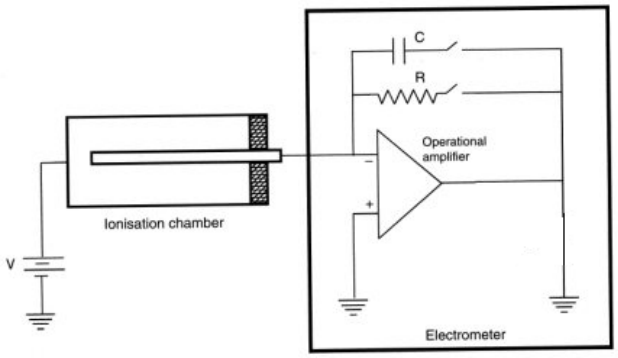

Figure 9: *The principle of negative-feedback operational amplifier electrometer* [18].

given in two different treatment planning systems.

An ionization chamber was used to perform the measurements, and an electrometer was used to measure the charge. Equation (2) is used to calculate from the charge to the absorbed dose in water, $D_{W,Q}$, for radiation quality Q [18].

$$D_{W,Q} = M_Q N_{S,Q_0} f_{Q,Q_0}^{D,S} \tag{2}$$

Here N_{S,Q_0} is the calibration factor in terms of a radiation quantity, S, in a beam of a standard quality, Q_0. This calibration factor is provided with the chamber. M_Q is the electrometer reading, suitably corrected in the user's beam. $f_{Q,Q_0}^{D,S}$ is any overall correction factor necessary to convert both from the calibration quantity, S, to dose, D, and from the calibration quality, Q_0, to the user's quality, Q [18].

Correction factors To calculate the correct dose rate in water, correction factors have to be applied. IAEA TECDOC [19] describes methods for obtaining the correction factors in brachytherapy.

The *polarity effect* comes from reversing the polarity on an ionization chamber. This means making the central node +V with respect to the wall and then change it to -V. In this case the correction factor for this effect is 1, since the effect is practically negligible for high-energy photons.

Charge will be detected that does not stem from the source itself, and this *noise* should be removed. For correction, charge detected was accumulated without the source in place, and this value was subtracted from the measurements.

The charge measured by an ionization chamber is dependent on *pressure*, *temperature* and *humidity*. When calibrating the chamber, the calibration factor must be given for stated reference values of these parameters. Most calibrations factors refer to $T_0 = 20\,^{\circ}\mathrm{C}$ and $P_0 = 101.3\,\mathrm{kPa}$. A correction factor should be applied to convert the measured charge to the reference conditions used for the ionization calibration. Calculation of this correction factor, k_{TP}, is shown in

equation 3. Here P_0 and T_0 are the reference values and P and T is the actual pressure and temperature when performing the measurements.

$$k_{TP} = \frac{(273.2 + T)}{(273.2 + T_0)} \frac{P_0}{P} \tag{3}$$

Calibrating the chamber is done without humidity correction, but the relative humidity during calibration is controlled within the range of 45-55%. The calibration factor applies for relative humidity around 50%, but in practice no correction factor is required from 20 to 70%. Therefore the correction factor for humidity, k_{hum}, is equal to 1.

The *recombination* of positive and negative ions within the air cavity reduces the amount of charge collected. At St. Olavs Hospital this correction factor, k_{recomb}, has been measured to be equal to 1.

A *calibration factor*, N_k, for air kerma rate is provided for the ionization chamber. This factor applies when the temperature, pressure and humidity is as stated previously.

Stopping power is defined as average energy loss per unit distance, S_{col}/ρ. This is dependent of the medium. Determination of absorbed dose in a medium using an ionization chamber is based on a principle (Bragg-Gray) relating the absorbed dose at a point in the medium (water) to the mean absorbed dose in the detector (air) through a proportionality factor: ratio of mass (collision) stopping power, $S_{w,air}$. For ^{192}Ir the *stopping power ratio* is 1.11.

For comparison between measurements with different radiation/accumulation time, it is more convenient to discuss dose rate than dose, and therefore the radiation time, $t(s)$, is also included in the formula.

Equation (2) can then be written as shown in equation (4), in terms of dose rate, $\dot{D}_{W,Q}$.

$$\dot{D}_{W,Q} = \frac{M_Q}{t} N_K S_{w,air} k_{pol} k_{TP} k_{recom} k_{hum}, \tag{4}$$

The unit is Gy/s and M_Q is corrected for noise and polarity [18] [19].

To be able to compare the dose rate with the treatment planning system, or measurements done on different days, it is important to include the date of the actual measurements or treatment planning, since the source decays. It is common to calculate the dose rate as if the measurements where done on the calibration date, and a decay factor is then needed. This is shown in equation (5).

$$F_{decay} = e^{-ln2 \cdot t/t_{\frac{1}{2}}}, \tag{5}$$

where $t_{\frac{1}{2}}$ is the half-life of the source and t is the time since the calibration date. Equation (6) then gives the dose rate, if it were to be measured on the calibration date. A decay table for the source is ofteen included when a new source is delivered.

$$\dot{D}_{W,Q}(0) = \frac{\dot{D}_{W,Q}(t)}{F_{decay}} \tag{6}$$

A calculation example of charge to dose rate in water is shown in appendix A.

2.3 3D treatment planning

2.3.1 Formalism of Task Group No 43 (TG-43)

Treatment planning and dosimetry has not developed at the same rate for brachytherapy as for that of external beam radiotherapy. The same relatively simple algorithms and calculation procedures have been in use for many years, not having any accurate dosimetry system available. Recently there has been some new developments associated with brachytherapy treatment. Increased availability of CT scan data, use of MR-images for volume definition and the use of Monte Carlo methods for dose calculation are some examples. These new developments have led to an increased interest for improved accuracy of brachytherapy dosimetry [6].

The Radiation Therapy committee of the American Association of Physicists in Medicine (AAPM) formed Task Group No 43 (TG-43) in order to review the different publications on the dosimetry of interstitial brachytherapy sources. They recommend a dosimetry protocol including a formalism for dose calculation and a dataset for the values of dosimetry parameters [6] [20].

Traditionally, the dose rate, $\dot{D}(r)$, at a distance r from an interstitial brachytherapy source was calculated using a point-source approximation. One problem with the older protocols is that they are based on photon fluence around the source in free space, not considering a scattering medium around the source (e.g. a patient) when calculating the dose distribution. In the recommended formalism this problem is solved by the use of measured dose distribution produced by a source in a water equivalent medium.

The recommended formalism allows for two-dimensional dose calculations around cylindrical symmetrical sources, whereas the old protocol could only handle one-dimensional point isotropic sources. The geometry of the formalism is defined in a polar coordinate system, with its origin in the source center and the angular origin in the longitudinal axis of the source. This is visualized in figure 10.

The dose at a point P(r,θ) in figure 10 can then be expressed as shown in equation (7).

$$D(r,\theta) = S_k \Lambda t \frac{G(r,\theta)}{G(r_0,\theta_0)} g(r) F(r,\theta) \tag{7}$$

Here r is the radial distance from the center of the source and θ is the polar angle with respect to the longitudinal axis. The reference point, $r_0\theta_0$, is located at $r_0 = 1$ cm, $\theta_0 = \frac{\pi}{2}$.

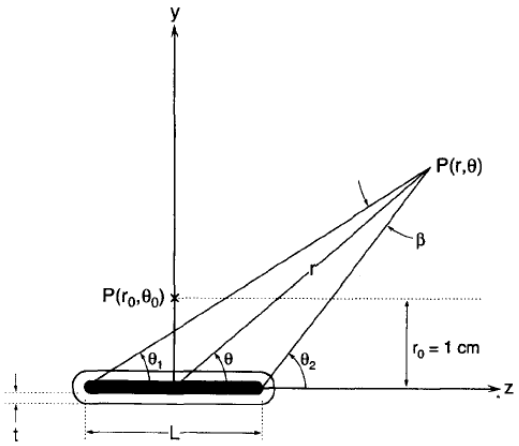

Figure 10: *Illustration of the geometry assumed in the formalism recommended by TG-43. $P(r_0, \theta_0)$ is the reference point* [20].

S_k is air kerma strength, defined as the product of air kerma rate and the square of the calibration distance, with units $\mu\text{Gy} \cdot \text{h}^{-1}\text{m}^2$. AAPM recommends that sources should be specified in terms of S_k [21].

Further, Λ is the dose rate constant and t is the exposure time. $G(r, \theta)$ is the geometry factor accounting for the dependence of photon fluence around a source in free space. $F(r, \theta)$ is the anisotropy function and accounts for anisotropy of dose distribution produced by a source in a scattering medium. $g(r)$ is the radial dose function that includes the distance dependence of absorption and scatter in water along the transversal axis of the source.

The formalism recommended by this group has found broad acceptance and is now commonly used to describe the dose distribution of new and existing brachytherapy sources. It is the basis of many treatment planning systems, i.a. Masterplan and Plato used in this study.

2.3.2 3D treatment planning systems

A 3D treatment planning system can import CT and MR-images of a patient. In the images it is possible to see and thereby delineate anatomical structures of interest. The applicator can also be visualized in the image. Dose distribution is calculated without considering the applicator extent, but the applicator position is delineated in the image to define where the source can be positioned.

From the information visualized it is possible to manually create an optimized treatment plan, adjusting source positions and dwell time in each position. The system can then calculate the doses received in different volumes.

Plato planning system The treatment planning system currently used at St. Olavs Hospital for creating treatment plans for brachytherapy of cervical can-

cer is Plato planning system (Plato Brachytherapy Planning System v. 14.2.6) [22]. This has been in use since 2005.

Masterplan Since 2004 Masterplan (Oncentra Masterplan (Nucletron) v. 1.5) has been used when making treatment plans for external radiotherapy at St. Olavs Hospital, and recently a module for brachytherapy has become available [22]. Until now Masterplan has been used during brachytherapy only to draw the structures of interest, before exporting the images to Plato for further treatment planning. Now it was of interest to evaluate the possibility for carrying out all parts of brachytherapy treatment planning in Masterplan. A screen shot of Masterplan in the brachytherapy module is shown in figure 11.

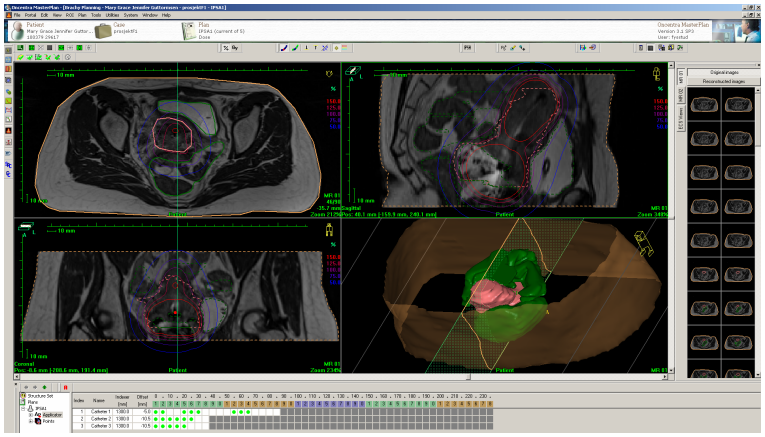

Figure 11: *A screen shot of Masterplan in the module used for brachytherapy planning*

2.3.3 Dose Volume Histogram

To evaluate dose to target, normal tissue and OARs, values of interest can be extracted from dose volume histograms (DVHs) of 3D treatment plans. A DVH shows how much dose different volumes of an organ receives. An example of a DVH is shown in figure 12. For comparing the overall dose delivery to a number of different structures of one particular treatment plan, the cumulative histograms for each of these structures are useful [3]. The volume receiving a given dose, minimum dose in a given volume and dose to the OARs can be found from DVHs.

Finding parameters of interest The volume of CTV receiving the presribed dose (in this study 5 Gy), CTV V100, is found from the DVH as shown in figure 12.

The minimum dose in 90% of the volume, CTV D90, is found by calculating 90% of the total volume of CTV, and then using the graph to find the minimum dose in this volume.

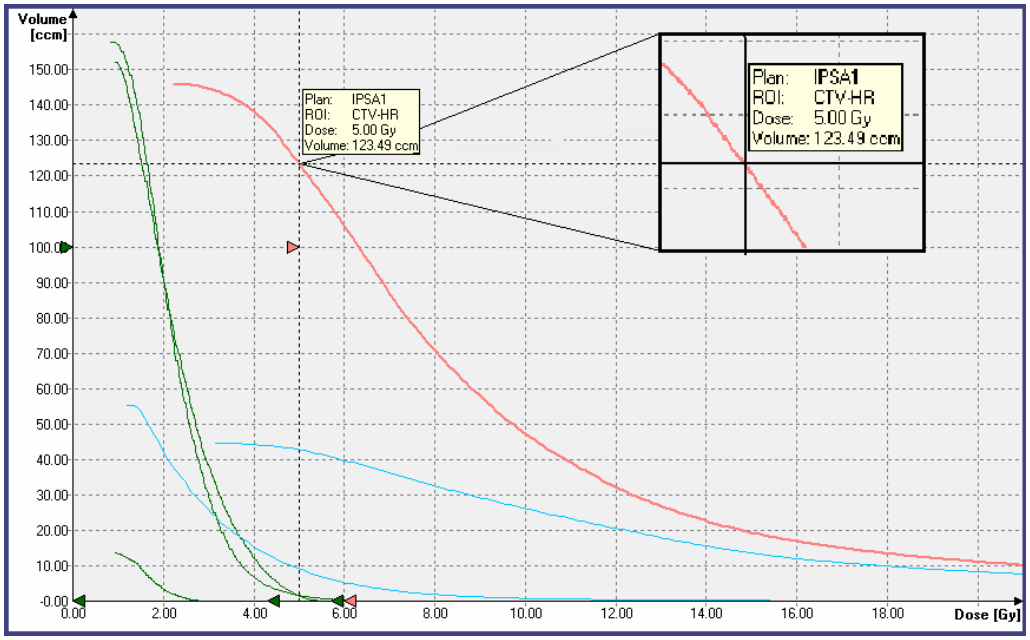

Figure 12: *Example of a cumulative* DVH. *The y-axis represents the volume* (cm^3) *and the x-axis represents the dose* (Gy). *The pink graph is the* CTV, *the green graphs are the three* OARs *and the blue graphs are the non-tissue material within and outside* CTV. *In the outlined square* CTV *V100 is read out. The external contour is not visualized in this* DVH.

The normal tissue receiving the prescribed dose, EXT V100, is found using the graph for the external contour, finding the volume receiving the prescribed dose. Then CTV V100 is subtracted to obtain the volume of the normal tissue.

2.3.4 Inverse planning simulated annealing (IPSA)

Simulated annealing is a method for locating a good approximation to the global minimum of a given function in a large search space, often used when the search space is discrete. The goal should be to find an acceptable solution in a fixed amount of time [23].

Inverse planning simulated annealing (IPSA) make use of the simulated annealing algorithm to find a good treatment plan for a given patient based on a set of dose constraints.

In order for IPSA to work, structures of interest must be delineated, such as target volumes and organs at risk. Then dose constraints and weighting factors can be given to each structure. Dose constraints can be given as both volume and surface restrictions to the structure.

In figure 13, the IPSA dialog box in Masterplan is shown. Here minimum and maximum dose to either volume or surface of the structures and appurtenant weighting factors are set. The example in the figure is shown in table 1. IPSA searches for the best possible solution that conforms to the given dose constraints by making different solutions by adjusting the dwell times in each position. The dwell positions are automatically generated by IPSA.

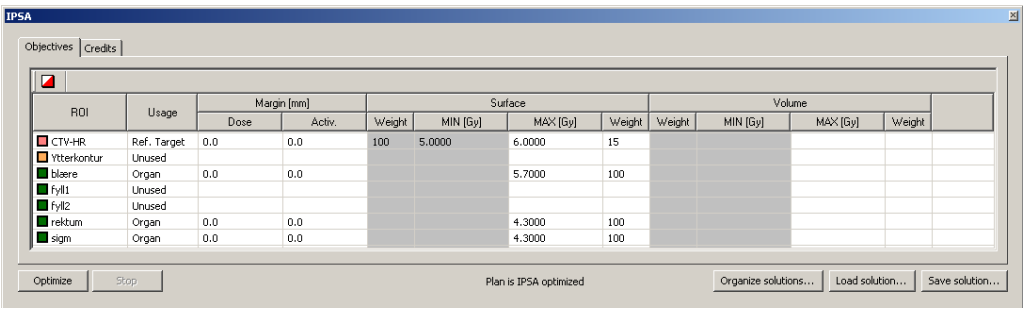

Figure 13: *The dialog box for* IPSA *in Masterplan.*

Table 1: *An example of a set of dose constraints with appurtenant weighting factors.*

	Dose_{min}	Weight	Dose_{max}	Weight
Target surface	5	100	6.0	15
Bladder surface			5.7	100
Rectum surface			4.3	100
Sigmoid surface			4.3	100

The weighting factor (M_{min}, M_{max}) sets the slope of the penalty function. If dose constraints are violated, the penalty will increase at the given rate. This is visualized in figure 14.

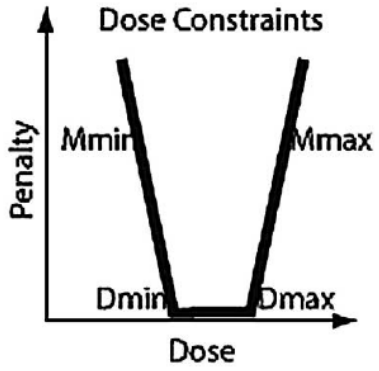

Figure 14: *Allowable range of dose and an assigned penalty for violating that range. D_{min} and D_{max} are the minimum and maximum dose, and M_{min} and M_{max} are the slopes of the penalty for violating minimum and maximum dose constraints, respectively* [5].

The best treatment plan will be the plan with the least amount of penalty [5]. For IPSA to find this treatment plan, the dose constraints are described mathematically.

The total dose, D_i, at point i is calculated by summing the dose contribution from all source positions, j, with their respective dwell time, t_j, as shown in equation (8). d_{ij} represent the dose rate at point i from the source position j.

$$D_i = \sum_j d_{ij} \cdot t_j \tag{8}$$

The penalty value, W_i, for each dose point generated by the algorithm can then be found as shown in equation (9) .

$$W_i = \begin{cases} M^{min}|D_i - D^{min}| & \text{if } D_i < D^{min} \\ M^{max}|D_i - D^{max}| & \text{if } D_i > D^{max} \\ 0 & \text{if } D^{min} \leq D_i \leq D^{max} \end{cases} \tag{9}$$

The sum of penalty values over all dose points leads to the global penalty known as the cost function, shown in equation (10). The sum is applied over all dose points, i, of each type, m, (volume or surface) for each defined volume, z. This determines the quality of dose distribution. A smaller global penalty value means that the treatment plan is closer to ideal dose distribution [24].

$$CF = \frac{1}{N^{volumes}} \sum_z \left(\frac{1}{2} \sum_m \left(\frac{1}{N_{mz}^{points}} \sum_i W_{imz}(t_j) \right) \right) \tag{10}$$

The IPSA program is combination of two parts. A user-to-computer translator that gathers the anatomic dose constraints given by the physician and an optimization engine that finds the best solution to fulfill the dose constraints.

2.4 Evaluation of treatment plans

Generally a 3D treatment plan for radiotherapy can be evaluated by means of indexes containing information about how well the target volume is covered, to which level normal tissue is irradiated and how well the given tolerance limit of the OARs is kept. It is also of interest to be able to distinguish between these three factors. For brachytherapy of cervical cancer it is difficult to include the bladder, rectum and sigmoid in such an index [1]. Use of 2D plots is therefore suggested with evaluation indexes versus the minimum dose in the 2 cm^3 volume receiving the highest dose ($OAR_{D2\,cm^3}$). This plot makes it possible to include the OARs and to gain more information on the quality of the treatment plan.

In this study, three indexes have been used for evaluation, TC (target coverage), COIN (conformal index) and COIN(weight) (COIN including a weighting factor for the irradiated normal tissue to emphasize the target coverage. The weighting factor equals 0.5 in this study). All indexes give values between 0 and 1, where 1 is the best possible value. The three indexes are shown in equation (11) [25], (12) [26] and (13) [27], a definition of the volumes used is shown in figure 15 and the abbreviations are listed below.

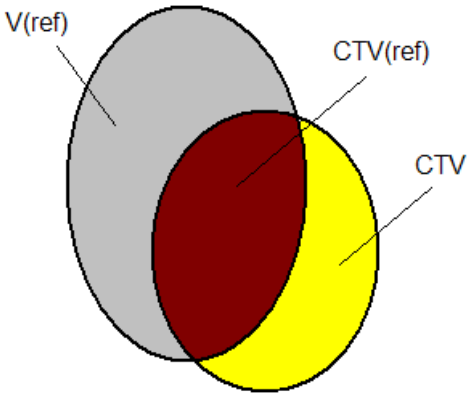

Figure 15: *Illustration of the volumes used in the indexes.*

$\boldsymbol{CTV}$ Clinical target volume (cm^3)

$\boldsymbol{CTV}_{ref}$ Clinical target volume receiving the prescribed dose or more (cm^3)

$\boldsymbol{V}_{ref}$ Volume receiving the prescribed dose or more (cm^3)

$$TC = \frac{CTV_{ref}}{CTV} \tag{11}$$

$$COIN = \frac{CTV_{ref}}{CTV} \cdot \frac{CTV_{ref}}{V_{ref}} \tag{12}$$

$$COIN(weight) = \frac{CTV_{ref}}{CTV} \cdot \left(1 - 0.5\left(\frac{V_{ref} - CTV_{ref}}{V_{ref}}\right)\right) \tag{13}$$

3 Methods and materials

3.1 Brachytherapy of cervical cancer

3.1.1 Treatment

At St. Olavs Hospital ICBT is administered with a remote afterloading machine (GammaMed12i, see figure 16). GammaMed afterloader can be connected to an applicator placed in the treatment position near the target volume of the patient. Before brachytherapy of cervical cancer, the applicator is fitted in place in the uterus/vagina region during anesthesia by the physician, and the position is maintained by vaginal packing. The applicator used is a Titanium Fletcher style applicator with flexible geometry from Varian medical system. The source is placed in the applicator by the remote afterloading machine after the personnel has left the treatment room. The source used is a ^{192}Iridium source with a diameter less than 1 mm. It is used as a stepping source, meaning that it is placed in the defined source positions for a certain amount of time (dwell time). The individual source positions and dwell times are specified by the treatment plan.

Figure 16: *The remote afterloading machine used at St. Olavs Hospital, GammaMed 12i* HDR.

The cervical cancer patients included in this study received external radiation therapy combined with brachytherapy of the cervix area as a boost. From the external treatment the patients received 50 Gy in 2 Gy fractions. For the ICBT treatment, the patients were treated with 4 fractions, 5 Gy per fraction. 11 patients treated at St. Olavs Hospital between 2007 and 2009 are the basis of the retrospective evaluation in this study. The use of the data have been approved by the patients and the ethical committee at St. Olavs Hospital.

3.1.2 Regions of interest (ROI)

For each fraction of brachytherapy, MR-images are taken with the applicator inserted in the cervix area (MR-machine: Siemens Avanto 1.5 T, resolution equals 1 mm). The images are transferred to the dose planning system, Oncentra Masterplan version 1.5 (Nucletron). The following regions of interest are delineated in each of the images.

- Target volume
- OARs (Bladder, rectum and sigmoid)
- Non-tissue material (Applicator and vaginal packing)
- Body contour is automatically drawn in Masterplan

The physician delineates a target volume defined as the clinical target volume (CTV) including the tumor, cervix, infiltration of parametrium, upper part of vagina, lower part of uterus and preferably the whole endometrium. The surface of this volume should receive 5 Gy on average. The physician allows for original tumor spread, and the volume delineated is a modification of the definition of HR-CTV from GEC-ESTRO.

The rectum and the sigmoid are drawn in the MR-slices where the target volumes are drawn and in a few slices cranially and caudally of these. Therefore the detected total volumes of the rectum and the sigmoid in the dose planning system are smaller than the total volumes of these organs. The whole volume of the bladder is drawn. Before treatment the bladder is drained, and then filled with 100 ml 0.9% NaCl. The main reason for filling the bladder is that most of the bladder wall should be moved away from the target volume, thereby reducing the dose to a larger part of the bladder wall. If the bladder had been empty, the whole bladder wall would be closer to the target volume and thereby receive more radiation.

The non-tissue material includes the volume of the applicator/ovoids and the vaginal packing that is placed to maintain the position of the applicator. One structure is drawn for the non-tissue material lying inside the delineated target volume, and one for the volume outside. The volume of the non-tissue material has been excluded in all other volumes containing this, since these regions are of no clinical relevance. Removing the non-tissue material from the target- and normal tissue volumes makes the dose and volume values more clinical relevant, and more comparable to similar published data [13].

The body contour is used to obtain the total volume encompassed by the 100% isodose and other values concerning the adjacent normal tissue.

3.1.3 Treatment planning

Currently treatment planning is performed in the dose planning system Plato Brachytherapy Planning System v.14.2.6 (Plato) at St. Olavs Hospital (chapter

2.3.2). This system can import both CT and MR-images with the delineated structures.

The structures of interest are delineated in Masterplan, and then exported to Plato where the applicator and the source positions are defined. The uterine applicator and the two ovoids are reconstructed separately in the images. Reconstruction of the applicator in MR-images have been tested using phantoms at St. Olavs Hospital, and is accepted. Then a set of source positions in the applicators are defined. The distance between each possible source position in the applicators is 5 mm. The source positions lying inside the CTV are chosen to be active. A set of equally spaced dose points is also defined, lying on the surface of the target volume. The defined applicator and source positions are shown in figure 17. The computer calculates the dwell times in each source position, making the mean dose to the dose points equal to the reference dose. The isodose curves are visualized in the MR-images and dose to different volumes can be extracted from DVHs.

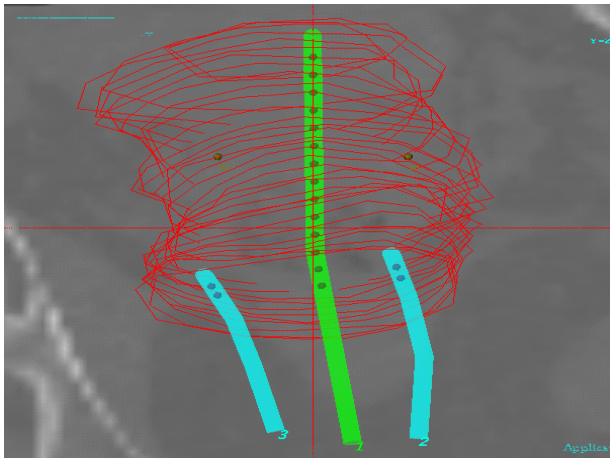

Figure 17: *Applicator and source positions visualized in Plato planning system (frontal view). The red structure is the delineated target volume.*

As discussed in chapter 2.1.6 the different OARs have specific limits for how much radiation they tolerate. These are not taken into consideration by the Plato planning system, but adaption is possible by manually altering dwell times and source positions. The tolerance dose per fraction used in the treatment at St. Olavs Hospital are calculated from the biological equivalent dose as shown in appendix B and are given in table 2. These calculations apply when 50 Gy is given by external radiation and ICBT is given in 4 fractions. The tolerance dose recommended by GEC-ESTRO for the total treatment has been used.

3.2 Comparison of dose calculations in Masterplan and Plato

To start the assessment on whether or not it is possible to use Masterplan instead of Plato for brachytherapy planning using the actual applicators, a comparison of

Table 2: The tolerance limits per fraction for $\mathrm{OAR}_{D2\,\mathrm{cm}^3}$.

OAR	*Tolerance limit per fraction* (Gy)
Bladder	5.7
Rectum	4.3
Sigmoid	4.3

the calculated dose distribution from the two programs was performed. Identical catheters were created in each of the computer programs, and the dose values at predefined points were read out and compared.

The difference (absolute values) between the doses calculated by Masterplan and Plato in each point is given as percentages of the dose calculated by Plato at that point. During the work, it was evident that this difference was larger in some regions than in others. In order to cover more precisely the areas with large errors, more points were read out in these regions. The difference in percentages of the calculated doses were then plotted, and the plots are shown in chapter 4.1. The coordinate system used in the plots is shown in figure 18.

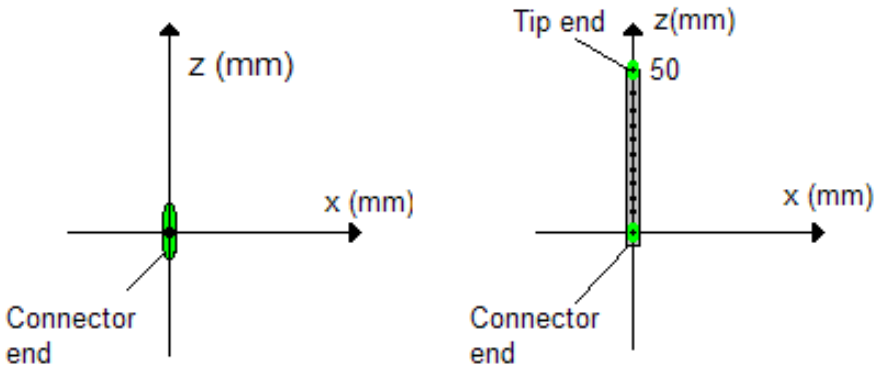

(a) Point source

(b) Straight catheter with 11 source positions

Figure 18: *The coordinate system used for the points compared in Plato and Masterplan. Only points for positive x have been used, since the treatment planning systems simulate a cylindrical symmetrical source.*

Measurements were performed simulating both a point source and a straight catheter with 11 source positions with equal center-center distance of 5 mm, and equal dwell times. The point source was situated in origo with the longitudinal direction of the source positioned along the z-axis. For the catheter, the points were evenly distributed between (0,0) and (0,50) mm.

3.3 Measurements of the GammaMed 12i HDR source

Measurements of the dose rate from the GammaMed source were performed for comparison with the dose calculations from Masterplan and Plato.

3.3.1 Measurement set-up

The measurement set-up is shown in figure 19 and included:

- Water phantom with a steering unit (Blue phantom and the software OmniPro accept (iba dosimetry))
- Ionization chamber (Farmer chamber FC65-G, calibrated for Iridium, $N_k = 43.8 \cdot 10^6$ Gy/C)
- GammaMed 12i HDR source and afterloader (the treatment unit at St. Olavs Hospital)
- 4 different catheters
- Electrometer (Scanditronix Wellöfer Dose 1)

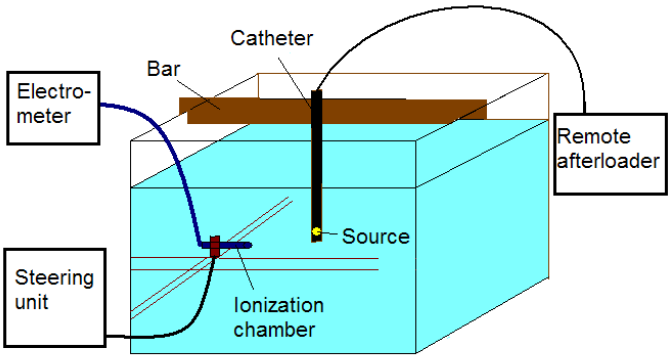

Figure 19: *Illustration of the measurement set-up.*

The ionization chamber was placed as shown in figure 20(a). The point source was positioned in origo in the coordinate system shown in figure 20(b), which also shows some of the points measured. All points measured are given in table 3.

Measurements were performed with the source placed in four different catheters: One catheter made of nylon (nylon), one being the Fletcher type ovoid catheter without a cap (ovoid) and two versions of the Fletcher type uterine catheter, one straight (StSt(straight)) and one slightly bent (StSt(bent)), both made of stainless steel. A picture of the different catheters used is shown in figure 21.

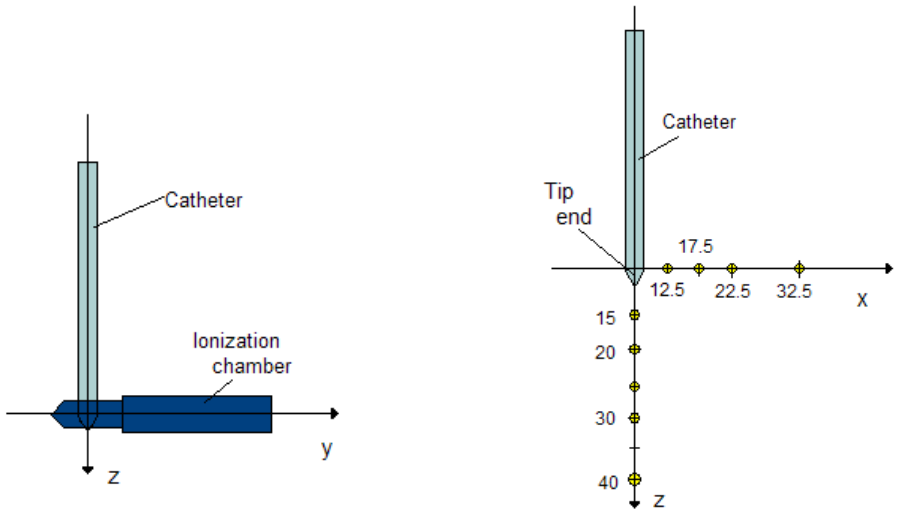

(a) (b)

Figure 20: *Illustration of the positioning of the ionization chamber (a) and the points measured (b).*

Table 3: *The points measured ((x,z) in the coordinate system in figure 20(b))*

x-axis (mm)	*z-axis* (mm)
(12.5,0)	(0,20)
(17.5,0)	(0,25)
(22.5,0)	(0,30)
(32.5,0)	(0,40)
(52.5,0)	(0,60)
(72.5,0)	(0,80)
(92.5,0)	(0,100)

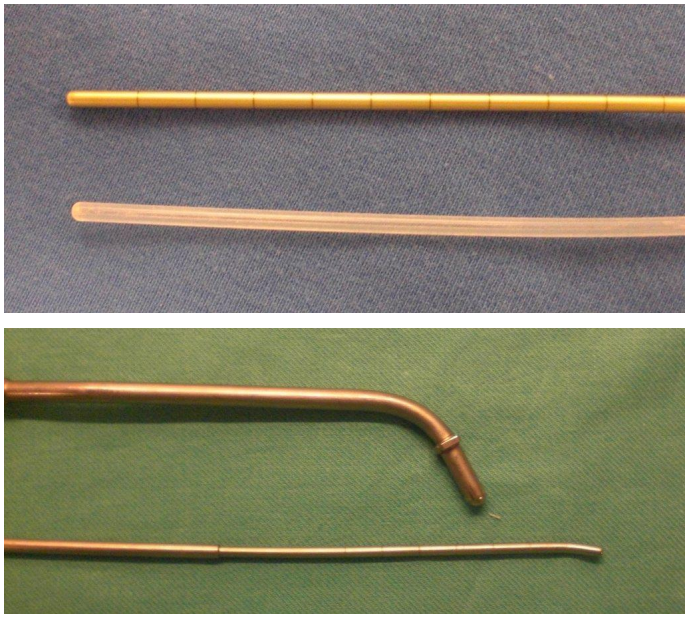

Figure 21: *The four different catheters used when measuring the source. From the top: StSt(straight), nylon, ovoid and StSt(bent).*

3.3.2 Measurement procedure

To be able to place the center of the source in the position defined as origo for every catheter, it was necessary to find the offset, i.e. distance from the tip of the catheter to center of the source placed in the position nearest to the tip. To find this offset the catheters were attached to a film (Gafchromic®EBT). The tip end of the applicator was marked on the film, and the film was radiated for 10 s. The distance from where the dose maximum was seen on the film to the marked tip end was measured. The offset was found to be 4 mm for nylon, 5 mm for StSt(bent), 5 mm for StSt(straight) and 10.5 mm for ovoid.

For the measurements the GammaMed 12i HDR source and remote afterloader was used. The catheter was placed in the water phantom and held in place by a bar positioned across the water phantom. The ionization chamber was placed in the steering unit and positioned with the center in the first point to be measured. Then it was connected to the electrometer. The catheter was connected to the afterloader, and after leaving the room, the source was placed in the catheter, radiating the ionization chamber. The charge detected was accumulated over a certain amount of time and displayed by the electrometer.

After measuring in one position, the ionization chamber was moved by the steering unit to the next position to be measured. This was repeated until all positions had been measured. For each position the accumulated charge was measured twice, and the average was used for further calculation. These measurements were performed for all four catheters.

The measurements were performed on different days. The accumulation time

for the first day was 60 s and for the second day 90 s.

An accumulation of charge detected was performed when the set-up was complete, without the source in place to find the noise. This was found to be 5.3 pC for 60 s and 8.6 pC for 90 s.

To be able to calculate the correct dose rate, actual temperature and pressure were measured both days.

The dose values calculated by Masterplan and Plato for the same positions as the ones measured were found simulating a point source in origo at the calibration date. The dwell time for the point source was read out and included in the calculations.

The measurements were converted from charge to dose rate (chapter 2.2.4) and the dose given in Masterplan and Plato were converted to dose rate. The values were plotted in excel, and are shown in chapter 4.2.

3.4 Comparison of treatment plans

3.4.1 Treatment plans

Different ways to create treatment plans are available in Masterplan. The algorithm, IPSA, is evaluated in this study.

Currently at St. Olavs Hospital, doses to OARs are not taken into consideration by the treatment planning program (Plato), and manual alteration of the dwell times to get a better dose distribution is time consuming. It is of interest to reduce the time spent on manual alteration. Therefore IPSA was tested to see if this algorithm, where dose restriction to OARs can be set, can give a better starting point for a treatment plan where less alteration is necessary.

Three IPSA plans with different dose constraints, free to optimize dwell times, and one plan with equal dwell times, where the dose was normalized to CTV, were made retrospectively for 11 patients. The four treatment plans were evaluated to see if one plan can give a better starting point than the others.

For treatment planning, the regions of interest had previously been delineated, but the applicator needed to be reconstructed, i.e. possible source positions in the applicator needed to be indicated. For the plan with equal dwell times, the source positions also had to be defined. These are evenly distributed (5 mm) along the applicator within the CTV. IPSA automatically generates the source positions within CTV, but adjustment of margins is possible in order to give IPSA the possibility to place the source outside CTV. In this study, this margin was set to 0, so all source position was placed inside CTV. Not all available source positions are necessarily used by IPSA.

For the treatment plan with equal dwell times, 200 target points situated on the target surface were calculated by Masterplan. Then the dose was normalized the mean of these points. For the IPSA plans, three sets of dose constraints were made, shown in table 4. To try to understand how IPSA generates a plan and to find solutions that can give a good starting point, different ways of matching constraints and weighting factors were tried on different patients initially. From

this trial and error method, three sets of dose constraints were suggested, and these are the ones to be evaluated.

Table 4: *Overview of dose constraints in the three different* IPSA *plans*

Plan	*ROI*	*Surface*				*Volume*	
		M_{min}	D_{min}	D_{max}	M_{max}	D_{max}	M_{max}
IPSA1	CTV	100	5 Gy	6 Gy	15		
	Bladder			5.7 Gy	100		
	Rectum			4.3 Gy	100		
	Sigmoid			4.3 Gy	100		
IPSA2	CTV	100	5 Gy	6 Gy	15		
	Bladder			7.0 Gy	100		
	Rectum			5.3 Gy	100		
	Sigmoid			5.3 Gy	100		
IPSA3	CTV	100	5 Gy	6 Gy	15	50 Gy	10
	Bladder			5.7 Gy	100		
	Rectum			4.3 Gy	100		
	Sigmoid			4.3 Gy	100		

IPSA1 At St. Olavs Hospital the delineated target should receive 5 Gy, so the first dose constraint sets minimum dose to the target surface to 5 Gy. The weighting factor for this is set equal to 100. Then a maximum dose to the OAR should be included. At St. Olavs Hospital they operate with a tolerance limit for a certain volume of the OAR given in table 2. Setting a constraint for such a volume is not possible in IPSA, therefore a maximum dose to the surface is used, i.e. no point on the surface of the organ should receive the given dose. For IPSA1 this was set to 5.7 Gy for the bladder and 4.3 Gy for the rectum and sigmoid. This is conservative since these values represent the tolerance limit for a small volume of the OAR. From experimenting with IPSA it seemed that the maximum dose to the organ surface sometimes was exceeded even though the dose constraints to the organ was included. It is not of interest to repeatedly have too high doses to the OARs in the starting point for the treatment plan.

For some patients, all OARs were situated at such distance from the target volume that the tolerance limits to the OARs were far from being exceeded. Then the surrounding healthy tissue received quite high doses since no limiting factor for this was available. A maximum dose of 6 Gy to the target surface was then considered. With a weighting factor of 15, this seemed to restrict the dose distribution somewhat, without decreasing the target coverage considerably.

IPSA2 Since maximum dose to the surface of the OAR in the previous suggestion is conservative, a higher maximum dose was tested. For IPSA2 the maximum dose to the surface of the OARs is set to be 7.0 for the bladder and 5.3 for rectum and

sigmoid (23% higher than for those given in IPSA1). The other dose constraints are the same.

IPSA3 For some patients large differences in dwell times were observed. To avoid this, a maximum dose to the target volume is tested. It seems like setting such a maximum dose will force IPSA to use more source positions. This might reduce the target coverage, so the weighting factor should not be large. A maximum dose to the target volume of 50 Gy, with the weighting factor of 10 is suggested. IPSA3 then equals IPSA1, with the addition of the maximum dose to target volume.

No manual alteration was done for any of the treatment plans.

3.4.2 Assessing the different treatment plans

In this study, 11 patients that have been treated at St. Olavs Hospital are included. The four treatment plans were made for the first fraction for the patients, except for one patient where the second fraction was used. The DVHs containing dose information of CTV, OAR, external contour and the two volumes of non-tissue material were exported to a data base made for this purpose. Values of interest were then extracted and calculated.

Statistical analysis In this study, four treatment plans are compared with respect to each other. When more than two means are compared, ANOVA (analysis of variance) can be used. This is the same as a two-sample t-test, comparing more means at once. When using ordinary pairwise comparison (several individual t-tests), too many significant differences between the sample means tend to be found.

Between-group-variations and within-group-variations are compared in ANOVA to assess whether there is a difference in population mean. Thus by comparing these two measures of variance with one another, true differences among the underlying group population means can be detected. If the variations between the sample mean is large, relative to the variation within the samples, it is likely to detect a significant difference among the sample means.

In this study tukey-intervals have been used for multiple comparison of dose and volume parameters for the four treatment plans. A 95% confidence interval was used for all values, resulting in a P-value equal to 0.05 [28].

Assumptions The underlying assumptions when using ANOVA are independence, equality of variance and normality.

The observations (patients) within each sample (11 patients with one treatment plan) should be independent and the samples should be independent of one another. For this study the observations within each sample is independent from the nature of the data, but since the samples include the same set of 11 patients, they are not independent of each other. This is called repeated measures, and ANOVA can be used for these cases in the same way as for independent ANOVA.

Both equality of variance and the normality assumption was checked, using Levene's test and Shapiro-Wilk test respectively. If there were no evidence against these assumptions, comparison with ANOVA could be performed. If there were evidence against one of these assumptions, the values were evaluated more carefully, and if necessary they were transformed. A logarithmic transformation was then performed and the equality of variance- and normality assumptions were checked again before executing the ANOVA comparison and finding the level of significance. ANOVA is robust to the normality assumption, and if the distribution is symmetrical and no gross outlier occur, transformation is not necessary. For one value it was necessary to remove one patient, due to one gross outlier.

The data was statistically analyzed in the computer program R [29].

4 Results

4.1 Comparison of dose calculations in Masterplan and Plato

It was of interest to compare doses calculated by Masterplan and Plato as one part of the evaluation of whether or not it is possible to use Masterplan in stead of Plato for treatment planning for the GammaMed source. Masterplan and Plato simualte different source types with slightly different geometry, and therefore deviations in the the two calculated dose distribution may occur.

A point source and 11 equally distributed source positions (catheter) was simulated in both Masterplan and Plato, and the dose calculated in different points around the source were obtained. The difference in dose calculated by Masterplan and Plato was found and is displayed in figure 22 and 23 as percentages of the point dose calculated by Plato. Absolute values are used for this plot, but both regions were the point dose calculated by Masterplan was higher than Plato and opposite was found. The corresponding data file is shown in table 9 in appendix C.

Point source There was one gross outlier in these measurements. Point (0,2) had a deviation of 126%. If this point is included, it is difficult to get any other information from the plot, and the point is therefore removed. In figure 22(a) the deviations in calculated dose around the point source between the two planning systems is shown.

This figure shows that no large errors occur further away than 5 mm from the source in x-direction. To get more information of the deviations around the source, a plot is made for $x \leq 5$ mm (figure 22(b)).

This plot shows that there is some deviation close to the source. More surprisingly it also shows large deviation below the connector end of the source ($x = 0$, $z \leq 0$).

In order to get more information about the distribution of the deviations, points with errors greater than 20% were removed. All of these points were situated close to the applicator or below the connector end. This leads to the plot shown in figure 22(c).

From this plot it is possible to say that no deviations greater than 3% occur further away than 4 mm from the points source (x-direction).

The deviations fall rapidly when moving in positive z-direction. No deviations greater than 4% occur further away than 7 mm from the center of the source.

Catheter with 11 source positions Comparison of doses calculated by Masterplan and Plato was also done simulating a straight catheter, with 11 equally distributed source positions with equal dwell times within the catheter, with 5 mm between each source position. The catheter was positioned on a line from (0,0) to (0,50). There were one gross outlier, positioned at (0,52) with a deviation of 123.7%. This point was removed with the same argument as for the point source.

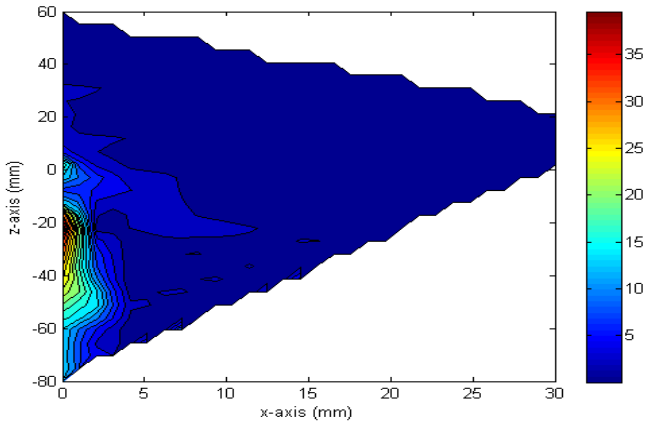

(a) Deviation around the point source when one gross outlier was removed.

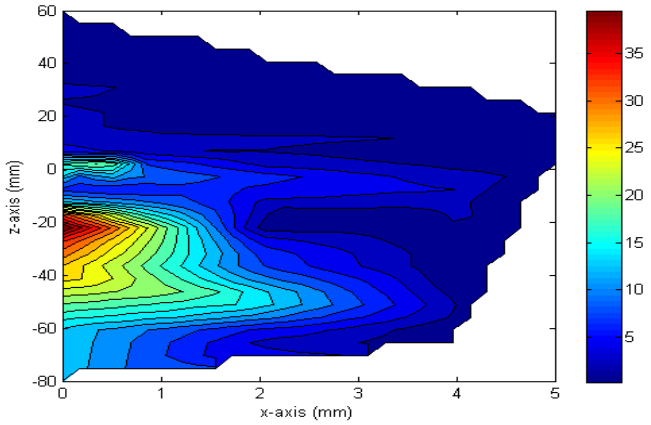

(b) Deviation around the point source when x $\leq$ 5.

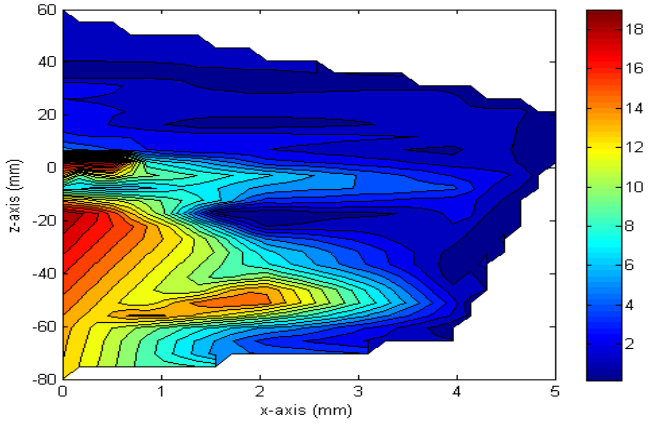

(c) Deviation around the point source when x $\leq$ 5 and the deviation larger than 20% has been removed.

Figure 22: *Deviations of doses calculated by Masterplan and Plato for a point source. The colorbar represents the deviation in percentages. The source is placed in (0,0), and the distribution of the deviations are shown in distance from the source (mm).*

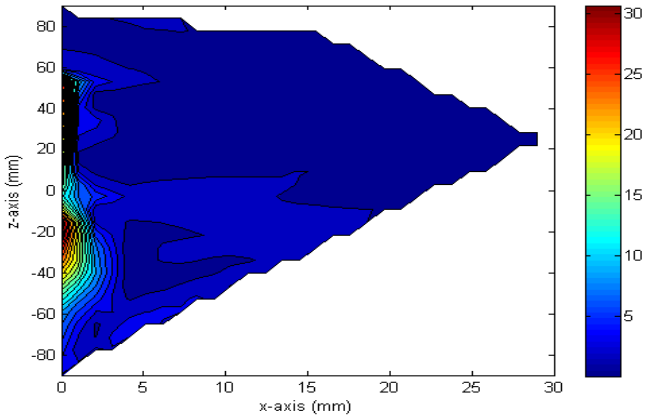

(a) Deviation around the catheter when one gross outlier was removed.

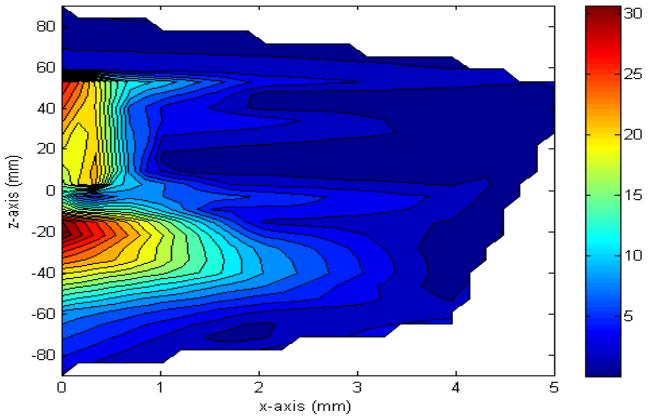

(b) Deviation around the catheter when x $\leq$ 5.

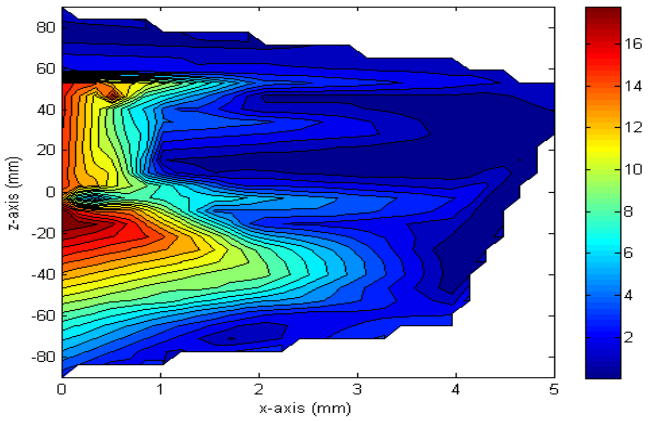

(c) Deviation around the catheter when x $\leq$ 5 and the deviation larger than 20% has been removed.

Figure 23: *Deviation of doses calculated by Masterplan and Plato simulating a catheter. The colorbar represents the deviations in percentages. The catheter is places from (0,0) to (0,50) with 5 mm between each source position. The distribution of the deviations are shown in distance from the catheter.*

The deviation between Masterplan and Plato for this case is shown in figure 23(a). From this plot it is possible to see that there are no large deviations more than 5 mm from the catheter in x-direction. The closer one get, the larger the errors, but it is difficult to read out any information of the distribution of the deviations close to the source. Therefore, a plot is made for x $\leq$ 5 mm (figure 23(b)).

It is evident that there are large errors close to the catheter and below the catheter in the connector end also for this case. To get more information of the deviations, the errors above 20% were removed. The result is shown in figure 23(c).

From this plot it is possible to say that no deviations larger than 4% occur further away than 4 mm from the catheter (x-direction).

The deviations fall rapidly in positive z-direction above the tip end. No deviations larger than 4% occur further away than 7 mm from the source center in the position closest to the tip end.

4.2 Measurements of the GammaMed source and comparison with Masterplan and Plato

It is of interest to measure the dose rate in points around a point source to compare the dose rates with dose calculations from Masterplan and Plato. The measurements were done with different applicators with various shape and material. The treatment planning systems calculate the dose distribution around the source disregarding the applicator. The points where measurements were taken, are given in chapter 3.3.1. The dose rate obtained from Masterplan and Plato are shown in figure 24.

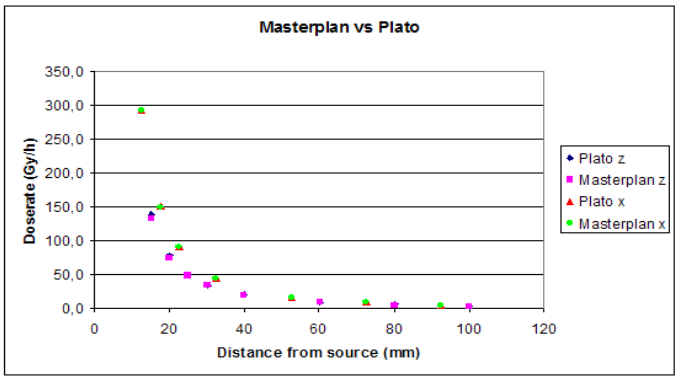

Figure 24: *Dose rate calculated by Masterplan and Plato in different distances from the point source. Masterplan z and Plato z means that the points measured are positioned along the z-axis. Masterplan x and Plato x are points lying along the x-axis.*

Calculation of dose rate values are similar for Masterplan and Plato in these points, therefore the measurements were only compared with calculations from

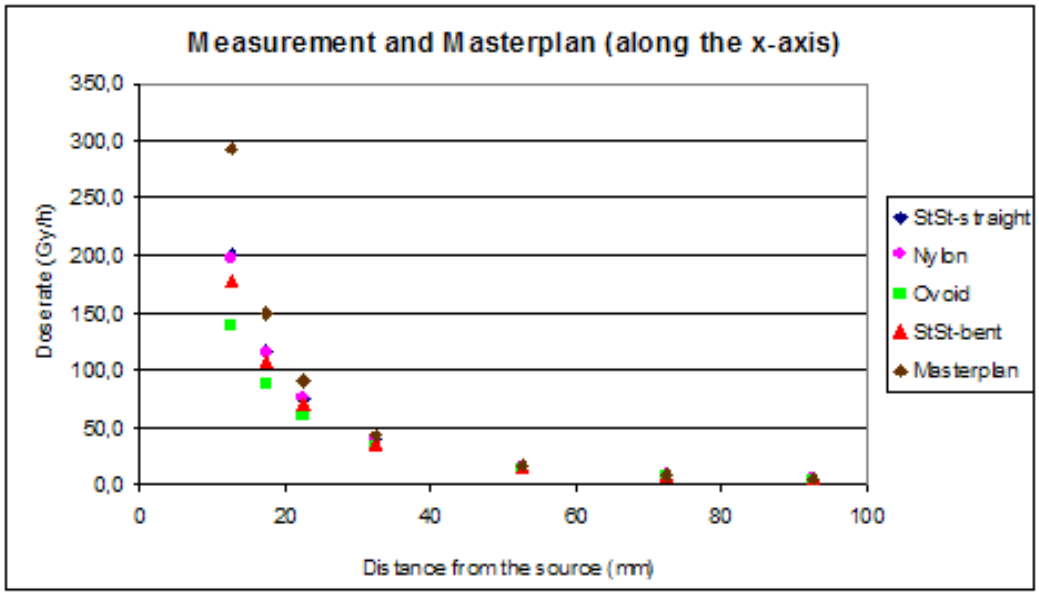

(a) Measurements of the points positioned along the x-axis.

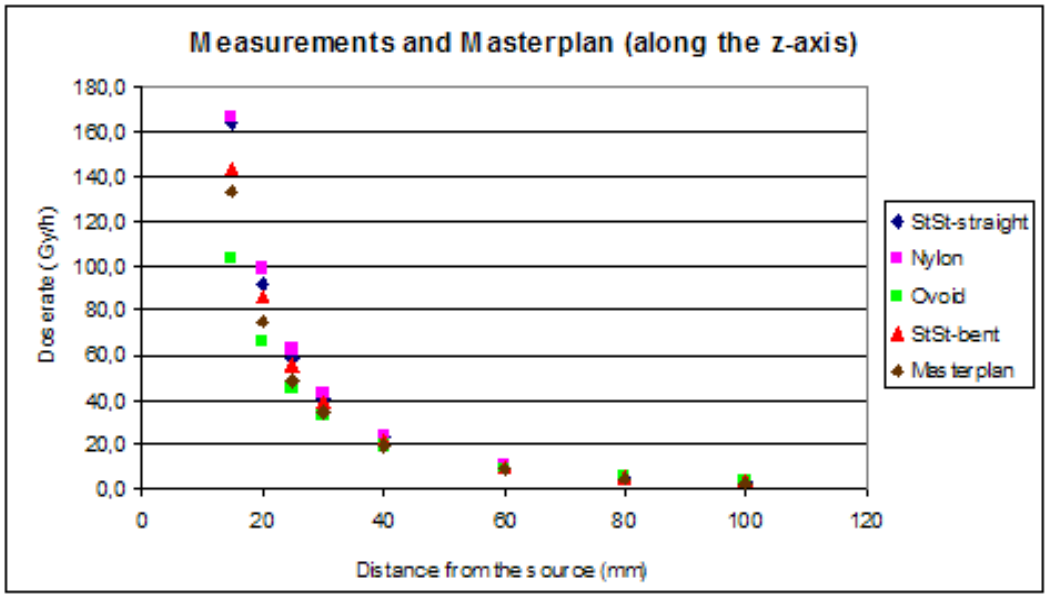

(b) Measurements of the points positioned along the z-axis.

Figure 25: *The dose rate from the measurements of the point source with different applicators and Masterplan as a function of distance from the source.*

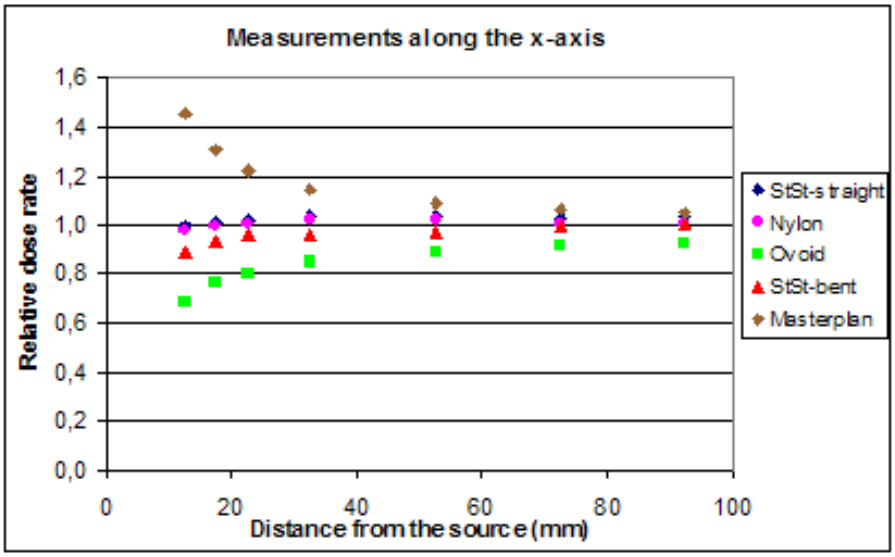

(a)

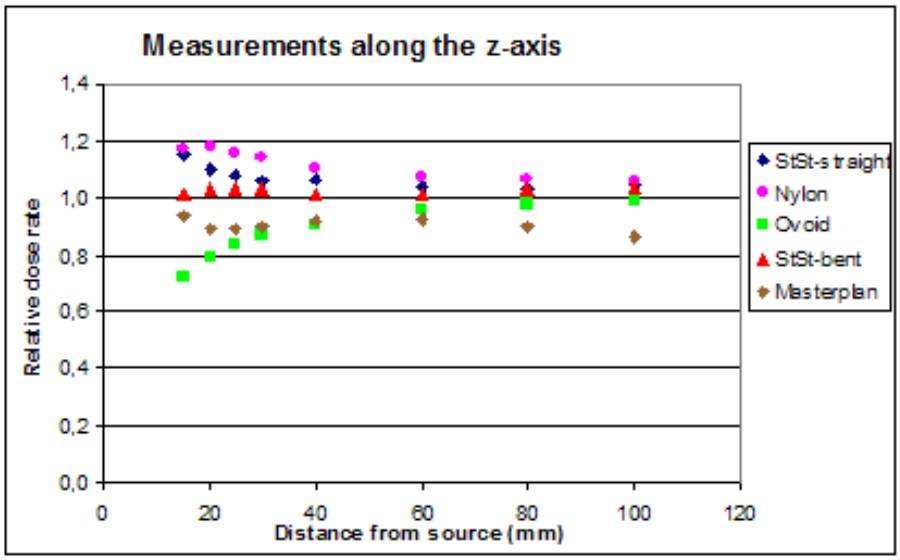

(b)

Figure 26: *Dose rate relative to mean dose rate from the measurements of the point source with different applicators and Masterplan, as a function of distance from the source.*

Masterplan. The results from the measurements are plotted in figure 25.

According to the plot, there are differences in dose rate at specific points both between the applicator types and between the measurements and calculations from Masterplan. The differences are more evident closer to the source. The measurements follow the same dose fall-off curve.

Dose rate relative to mean dose rate is plotted in figure 26. For the measurements along the x-axis these plots show larger deviations closer to the source. This also applies for the measurements in z-direction, even though it is not that evident. The plots also show that the deviations also occurs for measurements further away.

4.3 Comparison of treatment plans

4.3.1 Dose and volume means for the four treatment plans

The dose distribution from three different plans created by IPSA (IPSA1, IPSA2 and IPSA3) and one plan with equal dwell times (EDT) for 11 patients are evaluated. The results are shown in table 5. For most of the volume and dose means in the table, the values from IPSA2 are the highest and the values from EDT the lowest. In general, the values from IPSA1 are higher than the values from IPSA3.

Table 5: *The dose and volume means and standard deviations for parameters extracted from* DVH *and calculated parameters for the four treatment plans.*

		EDT	*IPSA1*	*IPSA2*	*IPSA3*
CTV	D90 (Gy)	3.2 ± 0.5	4.6 ± 0.8	5.3 ± 0.8	4.2 ± 0.8
	V100 (cm^3)	78 ± 32	99 ± 40	108 ± 41	95 ± 33
	V400 (cm^3)	6.0 ± 3.0	9.0 ± 5.7	10.3 ± 6.2	6.3 ± 3.3
EXT	V100 (cm^3)	19 ± 9.8	48 ± 29	71 ± 36	32 ± 9.2
OAR_{D2cm^3}	Bladder (Gy)	5.2 ± 0.9	5.4 ± 0.7	5.9 ± 0.6	5.1 ± 0.4
	Rectum (Gy)	2.6 ± 0.7	3.4 ± 0.7	3.7 ± 0.8	3.2 ± 0.6
	Sigmoid (Gy)	3.5 ± 0.9	4.3 ± 0.7	4.9 ± 0.8	4.2 ± 0.7
Indexes	TC	0.66 ± 0.07	0.84 ± 0.11	0.92 ± 0.06	0.81 ± 0.09
	COIN	0.54 ± 0.08	0.57 ± 0.09	0.56 ± 0.07	0.60 ± 0.07
	COIN(weight)	0.60 ± 0.07	0.70 ± 0.09	0.74 ± 0.05	0.71 ± 0.08

TC is 0.92 for IPSA2 which indicates satisfying coverage of target. For EDT, TC is 0.66, meaning that the target coverage for this plan on average is poor. Values for TC for IPSA1 and IPSA3 are similar, being 0.84 and 0.81 respectively.

The average for $bladder_{D2\,cm^3}$ and $sigmoid_{D2\,cm^3}$ for IPSA2 is 5.9 Gy and 4.9 Gy respectively. This is more than the tolerance limit for these two OARs.

The normal tissue receiving the prescribed dose, EXT V100, for IPSA2 is 71 cm^3 for IPSA2, while 19 cm^3 for EDT.

Statistical analysis A larger minimum dose in 90% of the volume (CTV D90) indicates better target coverage. For CTV D90 all three IPSA plans have significantly higher values than EDT, and IPSA2 has significantly higher values than IPSA3. No significant difference was found between the different plans for CTV V100 or CTV V400.

EXT V100 is the volume of the normal tissue receiving the prescribed dose, and this value should therefore be small. For EXT V100 IPSA2 has significantly higher values than IPSA3, and both IPSA1 and IPSA2 have significantly higher values than EDT.

Also for the $\text{OAR}_{D2\,\text{cm}^3}$, a smaller value is better. For rectum and sigmoid the dose evalutad is significantly higher for IPSA2 than EDT. For the bladder the only significant difference is found between IPSA2 and IPSA3, where IPSA2 has higher values.

For the indexes evaluated, a higher value signify a better plan. All three IPSA plans have significantly larger values for TC than EDT, and TC is significantly higher for IPSA2 than for IPSA3. No difference is found for COIN. For COIN(weight), all IPSA plans have significantly higher values than EDT. The P-values for these statements are given in appendix D.

4.3.2 COIN(weight) vs. OAR

COIN(weight) have been plotted versus $\text{bladder}_{D2\,\text{cm}^3}$, $\text{rectum}_{D2\,\text{cm}^3}$ and $\text{sigmoid}_{D2\,\text{cm}^3}$. The plot for the bladder is shown in figure 27. The plots for the rectum and sigmoid are found in appendix E.

Points to the right of the vertical line in the plot represent a plan where the tolerance limit of the OAR have been exceeded. The total mean of COIN(weight) for all four treatment plans is 0.69, and points above the horizontal line indicate that COIN(weight) for that plan is better than the average. Therefore, points in the upper left square signify a better plan. These points have been counted, and the results are given in table 6.

Table 6: *Number of treatment plans situated in the upper left square.*

	EDT	*IPSA1*	*IPSA2*	*IPSA3*
Bladder	1 (9%)	8 (73%)	4 (36%)	8 (73%)
Rectum	2 (18%)	8 (73%)	7 (64%)	8 (73%)
Sigmoid	1 (9%)	3 (27%)	2 (18%)	4 (36%)

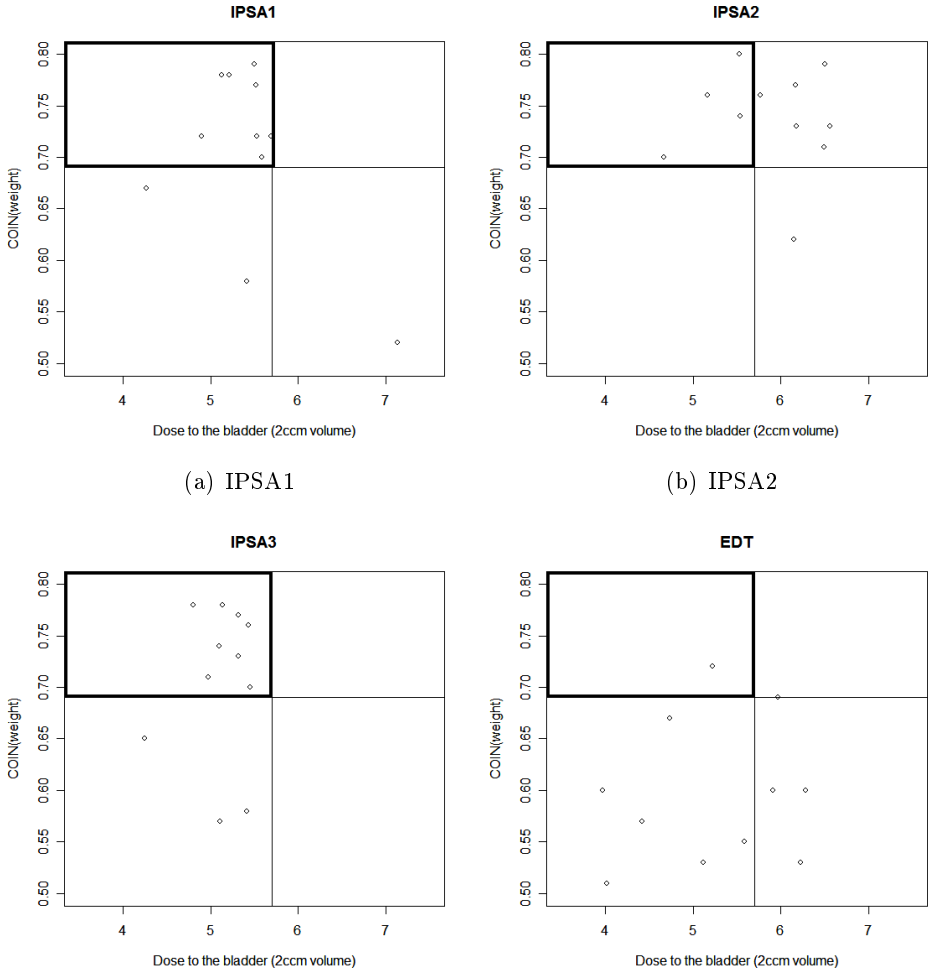

(a) IPSA1

(b) IPSA2

(c) IPSA3

(d) EDT

Figure 27: *COIN(weight) versus minimum dose in the volume* ($2\ \mathrm{cm}^3$) *receiving the highest dose for the bladder* ($\mathrm{bladder}_{D2\ \mathrm{cm}^3}$). *For points in the upper left square* COIN*(weight) is better than average and the constraints with respect to the* OAR *are fulfilled.*

4.3.3 OARs

Number of plans where the tolerance limit have been exceeded is also summed up from these plots. These numbers are shown in table 7.

Table 7: *Number of treatment plans where the tolerance limit for the given* OAR *have been exceeded.*

	EDT	*IPSA1*	*IPSA2*	*IPSA3*
Bladder	4 (36%)	1 (9%)	7 (64%)	0 (0%)
Rectum	0 (0%)	1 (9%)	3 (27%)	0 (0%)
Sigmoid	3 (27%)	6 (55%)	9 (82%)	4 (36%)
One or more OAR	5 (45%)	6 (55%)	9 (82%)	4 (36%)

4.3.4 Exclution of non-tissue material

In all values compared previously, the non-tissue material have been excluded to get a more representative evaluation. In table 8 some values have been calculated both including and excluding the non-tissue material to see what the differences is.

Table 8: *The difference in means for values extracted from* DVH *when including and excluding non-tissue material.*

Including		*edt*	*IPSA1*	*IPSA2*	*IPSA3*
CTV	D90	3.4 ± 0.6	4.8 ± 0.8	5.5 ± 0.8	4.4 ± 0.8
	V100	104 ± 40	127 ± 47	137 ± 48	123 ± 40
	V400	11 ± 5.7	16 ± 6.1	19 ± 7.0	13.6 ± 4.6
Indexes	TC	0.70 ± 0.06	0.86 ± 0.09	0.93 ± 0.05	0.85 ± 0.07
	COIN	0.56 ± 0.09	0.59 ± 0.10	0.58 ± 0.09	0.61 ± 0.08
	COIN(weight)	0.63 ± 0.07	0.73 ± 0.09	0.76 ± 0.05	0.73 ± 0.07

Excluding		*edt*	*IPSA1*	*IPSA2*	*IPSA3*
CTV	D90	3.2 ± 0.5	4.6 ± 0.8	5.3 ± 0.8	4.2 ± 0.8
	V100	78 ± 32	99 ± 40	108 ± 41	95 ± 33
	V400	6.0 ± 3.0	9.0 ± 5.7	10 ± 6.2	6.3 ± 3.3
Indexes	TC	0.66 ± 0.07	0.84 ± 0.11	0.92 ± 0.06	0.81 ± 0.09
	COIN	0.54 ± 0.08	0.57 ± 0.09	0.56 ± 0.07	0.60 ± 0.07
	COIN(weight)	0.60 ± 0.07	0.70 ± 0.09	0.74 ± 0.05	0.71 ± 0.08

5 Discussion

Dose calculations in Masterplan and Plato are based on absorbed dose in water, and do not consider variations in density of the tissue. The irradiated area in brachytherapy of cervical cancer consists mainly of soft tissue with high water content. Therefore this simplification does not lead to large dose differences when calculating the dose in water instead of soft tissue.

5.1 Comparison of dose calculations in Masterplan and Plato

The feasibility of using the Nucletron source type in Masterplan for simulation of the GammaMed source type used for treatment at St. Olavs Hospital is evaluated.

Since Plato planning system simulates the GammaMed source and Masterplan simulates the Nucletron source, comparing the dose distribution calculated by Plato and Masterplan will give information on how the dose distribution for the two source types differ. From figure 22 and 23 in chapter 4.1 differences in calculated dose are evident. Some of the differences are large, and are found in certain regions. It is important to evaluate these regions to see if these deviations is of importance.

During the treatment routine, assumptions are made in delineation of regions of interest and reconstruction of applicator. Small deviations in the calculations may be accepted.

For the point source one calculated dose point, positioned (0,2) mm from the center of the source, was removed from the plot. The deviation detected here was 126%. The uterine applicator has an extent of 3 mm in diameter and an offset in the tip end of 5 mm. The actual point would be positioned within the applicator. Deviations in this region will be of no clinical relevance. Also for the 11 source positions, a calculated dose point was removed (123.7% deviation). This point (0,52) was 2 mm from the source center in the tip end, which is within the uterine applicator, and of no clinical relevance.

Figure 22(a) and 23(a) show that the calculated dose deviations in a certain distance from the source are 2-3% and can be accepted. To get more information of the deviations found closer to the source, a plot was made for both the point source and the 11 source positions where $x \leq 5$ mm.

Large calculated dose deviations occur close to the source, and also below the connector end (along the z-axis) where the deviation is still evident several cm from the source center. According to Ballester [16], it is expected to find deviations in this region, but not as large as 30% as the plot indicates. In a clinical situation of brachytherapy of cervical cancer these regions will consist of vaginal packing and the applicator, i.e. deviations in this region is not relevant to the target volume or OARs. However, in other clinical situations than brachytherapy of cervical cancer, this region could be of relevance.

For further evaluation of the deviations in dose distribution calculated by Masterplan and Plato, all points with larger deviation than 20% were removed from the data file for the plot. These were all positioned close to the source or

close to the z-axis below the connector end, which is within the vaginal packing in brachytherapy of cervical cancer. Removing these points will give more information in areas of greater clinical relevance.

As found in chapter 4.1 deviations larger than 3% and 4% (point source and catheter respectively) are not found further away than 4 mm in x-direction. Since the applicator has a certain extent, and the vaginal packing is situated below the connector end, the points with larger deviation than 3-4% will be within or very close to this non-tissue material and have no clinical relevance for brachytherapy of cervical cancer. For the tip end, no large deviations are found further away than 7 mm from the source center (z-direction). With an offset of 5 mm, this will be close to the uterine applicator.

Only the positioning of the points have been discussed, and even if these are in regions with no clinical relevance, these points are situated within certain volumes, such as CTV and adjacent normal tissue. In intracavitary brachytherapy, dose fall-off is rapid, and doses close to the source are extremely high, making mean dose to CTV an irrelevant parameter to measure. It is more common to evaluate measures such as the volume receiving the prescribed dose or more for target and normal tissue or minimum dose in a certain amount of the target. These measures will not be affected by the deviations close to the source, due to the high dose in these points.

If evaluating volumes close to the uterine applicator, such as CTV V400, the dose deviations might have a clinical effect. Removing the non-tissue material from the calculations will then be recommended, since most points with considerable dose deviations are situated within this non-tissue material.

The dose deviations will not affect the calculated dose for the OARs, since OARs are at some distance from the uterine applicator. As previously discussed, calculated dose deviations here are negligible.

Deviations between dose calculations from Masterplan and Plato do not change significantly when calculating for several source positions instead of a point source. Deviations are found along the catheter and below the connector end for the catheter. For the point source deviations are found close to the source and below the connector end. This is in good agreement with that found in Ballester [16].

From this evaluation, it seems that using Masterplan and the Nucletron source type for simulating the GammaMed source will give reasonable results.

5.2 Dose measurements around the GammaMed source

Measurements of the dose rate from the GammaMed source were performed to compare the dose distribution to dose rates calculated by Masterplan and Plato.

From figure 25 in chapter 4.2 it is possible to see that when the chamber is positioned 30 cm or more from the source, the different measurements and the results from Masterplan are equal. This applies to both measurements along the x-axis and z-axis. Closer, deviations are found.

Small errors in the measurement set-up is difficult to avoid, particularly for the ovoid and the Stainless Steel(bent), since these applicators are curved. In

addition, the ionization chamber has a certain extent and the first position for measurement is positioned manually. Therefore 1-2 mm errors in the set-up is expected.

The dose fall-off is extremely rapid for the ^{192}Ir-source, e.g. the dose rate values from Masterplan decrease from 300 to 100 Gy/h over 10 mm. Therefore there was raised a question of how close (3D) to the point measured one could find similar values in Masterplan. A manually check was done. The average distance to agreement, i.e. distance from original point for measurement to a point in Masterplan with the same value, was found to be 2 mm. The deviations found can therefore be a consequence of measurement set-up. Due to the high dose fall-off close to the source, this effect is more pronounced for the measurement closer to the source.

According to the relative dose rate plots, deviations are found for all measurements, but they increase towards the source. Errors in measurement set-up will concern all measurements, but is more prominent when the dose fall-off is high.

Presumably the deviations detected come from errors in measurement set-up, and large deviations between the dose rate calculated by the computer programs and dose rate measured do not occur. Small deviations however would be difficult to detect. The calculated dose rate in Masterplan and Plato are within the uncertainties of the measurements.

Effect of using different applicators Dose measurements with the source placed in different applicators (difference in shape, thickness and material) were performed.

The measurements when using nylon and StSt(straight) applicators are similar. Due to the geometry of the applicators, the set-up for these two are probably more precise than for ovoid and StSt(bent), and this would lead to more correct measurements.

The lowest dose rate was found when using the ovoid applicator. The diameter of this applicator is 5.9 mm in diameter, while the diameter of the other applicators are 3 mm. The thickness of the applicator was not corrected for when positioning the ionization chamber. Measurements are therefore taken approximately 1.4 mm further away than for the other applicators. This can be the reason for the lower measurements.

Dose measurements from StSt(bent) applicator are between StSt(straight) and the ovoid. Positioning the ionization chamber correctly was difficult for the bent applicator.

The applicator material is not included in the dose calculations by Masterplan and Plato. For dose calculations along the x-axis, Masterplan has the highest values. This is expected, since Masterplan does not include attenuation in the applicator material. However, for the vertical values the measurements from StSt(straight), StSt(bent) and nylon are higher. Dose distribution calculated by Masterplan and Plato is not completely circular, but has the shape of an apple. The measurements along the z-axis are in the region of the slight dip in the dose

distribution in the connector end.

5.3 Comparison of different treatment plans

The aim of curative radiotherapy is to achieve tumor control while avoiding serious damage to surrounding structures. High target coverage often leads to more irradiated normal tissue and larger dose to the OARs, and a compromise between these factors is often necessary. Creating dose distributions more conformal to the target can give better target coverage without necessarily increasing the dose to surrounding structures.

A typical case is shown in figure 28. From this figure it is evident that positioning of the OARs determine the possibility for a satisfying target coverage.

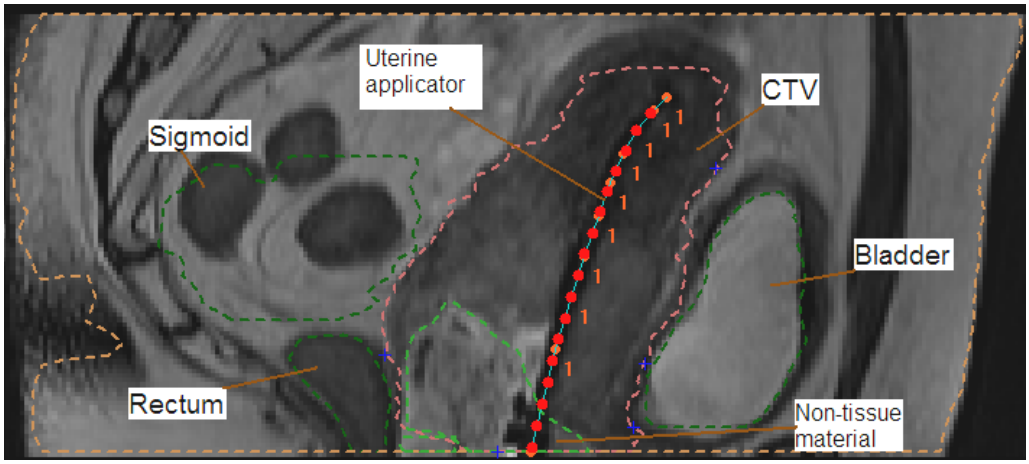

Figure 28: MR-*image (sagital view) of a patient with delineated structures, before creating the treatment plan. Due to the positioning of the surrounding* OARs *and the uniform shape of* CTV*, a plan with satisfying target coverage should be achievable for this patient.*

The treatment plans made by IPSA will not necessarily be satisfying for all patients, even though OARs are taken into consideration together with coverage of the CTV. The plans must be carefully examined and alteration may still be necessary [30]. The main goal for using this algorithm is to get a better starting point, in order to save time when preparing the treatment plan. Adjustment of the dose constraints for different patients will be time consuming and difficult. A set of dose constraints that can be used for every patient should therefore be found.

The mean values for target coverage, irradiated normal tissue and dose to OARs given by DVHs in table 5 differ, but from the statistical analysis fewer significant differences are found. As mentioned, 11 patients are included in this study, and for a better statistical analysis more patients would have been preferable. Even so, with the significant differences found, assessing the mean values and using the plots in chapter 4.3.2, evaluation of the treatment plans can be done.

A pattern for the mean values in the table is detected. For all values, with the exception of COIN and bladder$_{D2\,\mathrm{cm}^3}$, the value from IPSA2 $\geq$ IPSA1 $\geq$ IPSA3 $\geq$ EDT. This suggests that better target coverage also will lead to more irradiated normal tissue and larger dose to the OARs.

Target coverage Minimum dose in 90% of the target volume, CTV D90, the volume of CTV that receives the prescribed dose, CTV V100 and the index TC are all indicators of how well the target is covered. For these three factors IPSA2 has the highest value, indicating that this plan leads to best target coverage. EDT has the lowest values and will give the poorest target coverage.

Normal tissue A high target coverage is desired, but often this correlates with more dose to the surrounding normal tissue. EXT V100 is the volume of normal tissue receiving the dose prescribed for the target. IPSA2 has the highest value for EXT V100 and thus IPSA2 is the plan leading to most irradiated normal tissue. According to EXT V100, IPSA1 will irradiate more normal tissue than IPSA3 and EDT. Lowest amount of irradiated normal tissue is found when using EDT.

OARs In a treatment planning situation, it is usually the OARs that limit the target coverage. Dose to the OARs are of great importance when assessing these four treatment plans, because if the tolerance limit is exceeded, the plan must be altered. Figure 29 shows a case where bladder will limit the target coverage. Dwell times in the source position in close proximity to the bladder is forced to be low, for not giving too high dose to this OAR. This case will also probably lead to inhomogeneities in dwell time values, discussed later in this chapter. For a better target coverage, higher dwell time values will probably occur in the tip end of the applicator to compensate for the lower dwell time values closer to the bladder.

For both bladder and sigmoid the minimum dose in the 2 cm^3 volume receiving the highest dose (OAR$_{D2\,\mathrm{cm}^3}$) is higher than accepted for IPSA2. Average doses over the tolerance limit indicates that many plans will need adjustment. The average of OAR$_{D2\,\mathrm{cm}^3}$ is below the tolerance limit for the other plans. Since this limit is absolute, no plan should exceed the tolerance limit for any of the OAR. The average alone is therefore not representative for evaluating the OARs.

A more relevant way of evaluating the quality of a treatment plan when it comes to the dose to OAR, would be to examine how many of the treatment plans that exceed the tolerance limit for OAR$_{D2\,\mathrm{cm}^3}$. 82% of the plans from IPSA2 exceed the tolerance limit for one or more of the OARs. IPSA3 has the lowest amount of plans (36%) that need adjustment due to the OARs (table 7). Surprisingly this is better than EDT, which is said to be the conservative plan. This suggest that allowing the dwell time to conform to the shape of CTV will give possibilities for a better target coverage as well as less dose to OARs. This is visualized in figure 30.

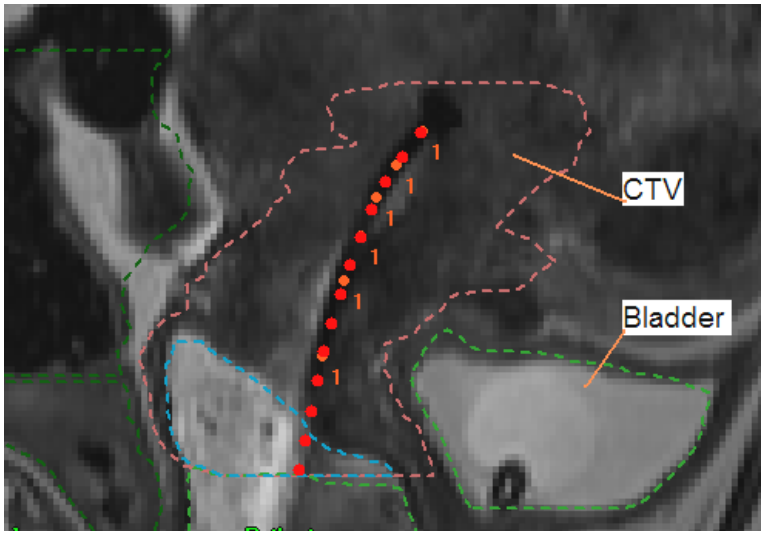

Figure 29: *For this patient the bladder is positioned in a way limiting the target coverage to be lowered. Dwell times in the lower part of* CTV *must be lowered not to exceed the tolerance limit.*

The dose constraints from IPSA1 are set in such a way that no points on the surface should receive a higher dose than 5.7 Gy for the bladder and 4.3 Gy for the rectum and sigmoid. These numbers are the tolerance limit for $\text{OAR}_{D2\,\text{cm}^3}$, and not what should be the maximum dose to the surface. The maximum dose to the surface was found when $\text{OAR}_{D2\,\text{cm}^3}$ was at the tolerance limit. This maximum dose to the surface was approximately 120% of the tolerance limit for $\text{OAR}_{D2\,\text{cm}^3}$, and is set as the dose constraints for OARs in IPSA2. Therefore it is surprising that this dose constraint repeatedly leads to too high doses for one or more of the OARs. It was also tried to set the weighting factor for the OAR constraint to 200 when testing IPSA, but this led to little change in the results. Keeping the dose constraints for OAR low are therefore suggested. This seems to correlate with the litterature, where they set the dose constraints for the surface of an OAR in the same range as the tolerance limit to the 2 cm^3 volume [31] [32].

When reading out values for OARs from the DVH, it is important to consider continuity in the 2 cm^3 volume. In a study like this, continuity of the high dose area of the organ is assumed, but not necessarily the case. When obtaining the dose in the 2 cm^3 volume from the DVH, there is no guarantee that this volume is continuous, and this method can lead to wrong conclusion when evaluating dose to these organs. An example where this is evident is shown in figure 31.

A manual inspection was done to see if there were any cases where it was clear that the 2 cm^3 volume was not continuous. For two patients the sigmoid had a shape like the one in figure 31 and the sigmoid was the limiting factor. For this case the 2 cm^3 volume is probably not continous. Restricting the dose distribution due to this will then be incorrect. One more patient had a sigmoid with the same shape, but here the dose to the sigmoid was far from the tolerance

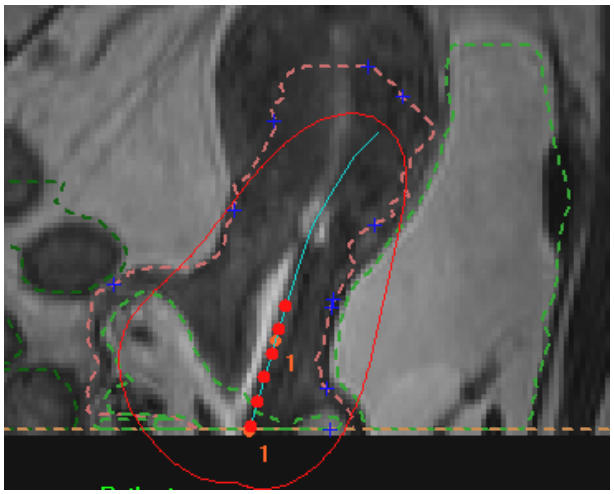

(a)

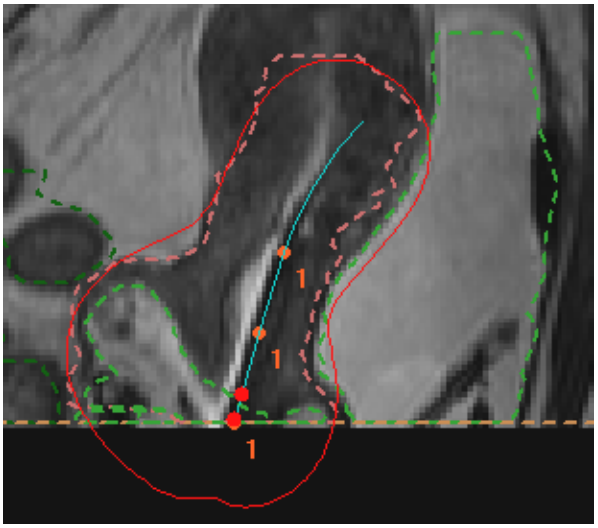

(b)

Figure 30: *An illustration of the effect of shaping the isodose lines, in order to get better target coverage in addition to less dose to the* OARs.

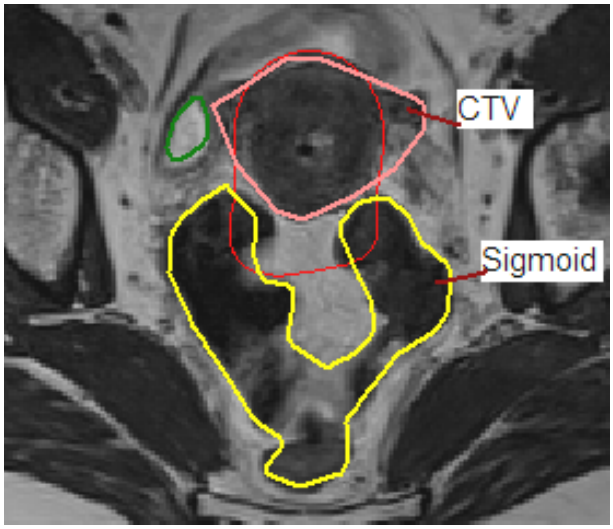

Figure 31: *An example where it is evident that the* 2 cm^3 *volume receiving the highest dose will not be continuous.*

limit. Then the plan would not be affected by the misleading read out. For the cases above it is clear that the volume is not continous, but for some cases it is difficult to see whether the volumes were continous or not.

Continuity is assumed, but not the case for all patients. International recommendation suggest that a part of an OAR receiving high doses should have a volume of 2 cm^3 before bearing clinical relevance. A better target coverage could have been achieved since a higher dose to the OAR could have been given without damaging the organ. For this study, all four treatment plans are made for the same patients, so comparing these plans with respect to each other will still be sufficient.

A worst case scenario is also assumed when calculating the tolerance limit per fraction: It is the same region of the OAR that receives the maximum dose for every fraction.

Indexes All indexes used in this study have values between 0 and 1, where 1 is the best possible value.

TC is an index giving information about how well the target is covered (equation (11)). This index has been discussed previously (target coverage). If the OARs are situated at a certain distance from the target, normal tissue might receive large radiation doses in order to improve target coverage. Therefore an index including normal tissue in addition to target coverage has been suggested [26]. COIN is such an index (equation (12)).

IPSA3 has little irradiated normal tissue, and since it has better target coverage than EDT it will be the best starting point for a treatment plan according to COIN.

Irradiated normal tissue is important to consider, but since three surrounding organs are monitored in particular, target coverage is of greater importance and

an index weighting target coverage and irradiated normal tissue equally can be misleading. A modification of COIN has been suggested, where a weighting factor is added to the term for normal tissue, emphasizing the target coverage. In this study, the weighting factor has been set to 0.5 (equation (13)).

IPSA1 and IPSA3 have similar values for COIN(weight). IPSA1 has the better target coverage and IPSA3 has less irradiated normal tissue. According to COIN(weight), IPSA2 is the best treatment plan.

Inhomogeneous distribution of dwell time values An inhomogeneous distribution of dwell time values was detected. This is not desired, and can lead to extremely high doses within CTV and for some cases outside CTV. An easily available measure for inhomogeneities in dwell time values is difficult to find. High dwell times in one source position will yield large doses around this point. CTV V400 is the volume inside CTV receiving 400% of the prescribed dose. It may therefore give an indication of inhomogeneities in dwell time values, and it is a measure of the unwanted effect resulting from these inhomogeneities. An example where one plan with equal dwell times and one plan where the dwell times differ considerably for one patient is shown in figure 32.

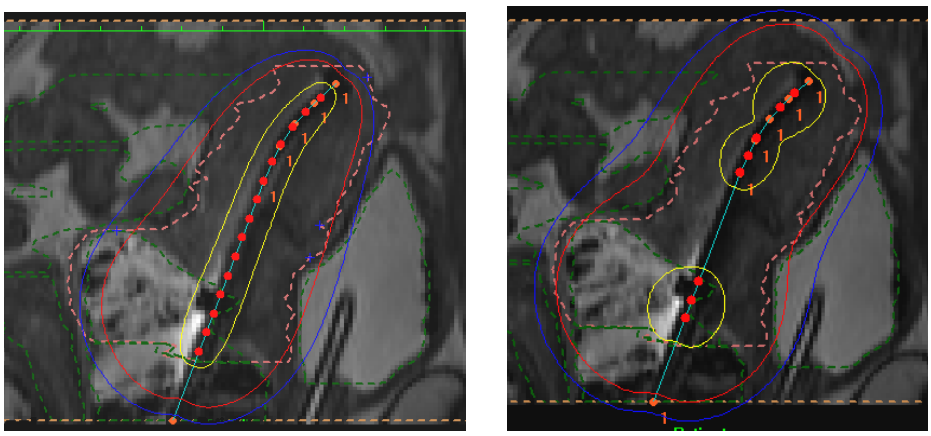

(a) Equal dwell times (b) Dwell times differ condiserably

Figure 32: *An illustration of how the shape of the 400% isodose line differs for equal dwell times and inhomogeneous distribution of the dwell time values. The yellow line is the isodose line for 400% of the prescribed dose, the red is 100% and the blue is 75% of the prescribed dose. The pink dotted line is the* CTV.

According to CTV V400, there are more inhomogeneities of dwell time values in IPSA1 and IPSA2. As expected, the volume is smaller for EDT, since for this plan the dwell time distribution is homogeneous. IPSA3 is a plan suggested to decrease the inhomogeneity in dwell time values. EXT V400 for IPSA3 is only slightly greater than EXT V400 for EDT, indicating that the maximum dose constraint had an effect.

Different suggestions have been proposed in order to obtain homogeneous dis-

tribution of dwell time values, but some of them are time consuming, which then removes some of the advantage of using IPSA. In this study, setting a maximum dose within the target volume was tested, and it seems like this lead to less inhomogeneity in dwell time values. This constraint does not lead to a homogeneous distribution, but from figure 29 and 30 it is evident that the possibility for shaping the dose distribution should be available. Inhomogeneous distribution in dwell time values is then inevitable.

A dwell time gradient restriction filter is available for a treatment planning system that is expected to produce solutions with smooth changes of dwell times along the catheter, preventing dominating source dwell positions. This should enable the creation of better security in the delivery dose distribution, without having to compromise to the optimization performance [33].

2D plots The four treatment plans have different advantages and disadvantages. One has better target coverage, another spares the OARs more. To be able to determine which treatment plan will give the best starting point for most patients, factors previously discussed should be considered in relation to one another. One plan might have poor target coverage due to nearby positioning of one of the OARs. Dose to OARs, target coverage and irradiated normal tissue all contribute in determining the quality of the treatment plan.

2D plots are suggested when assessing plan quality to obtain more information than using one index alone. A plot makes it possible to consider more factors, while still being able to separate them. COIN(weight) includes target coverage and irradiated normal tissue in a suitable way. This index is plotted versus $\text{OAR}_{D2\,\text{cm}^3}$, and this plot will provide much information on the treatment plan (chapter 4.3.2 and appendix E).

In the plots a vertical line is drawn, indicating tolerance limit for $\text{OAR}_{D2\,\text{cm}^3}$ in the given OAR. The horizontal line in the plots is the total mean for COIN(weight) for all four treatment plans (0.69). Points in the upper left square thus represent treatment plans that fulfill the dose constraints for the OAR and have a better COIN(weight) than the average.

More points in the upper left square will signify a generally better treatment plan, and in table 6 points in the upper left square have been summed up. When evaluating the information with respect to each other, it is evident that IPSA1 and IPSA3 will give better starting points for treatment planning. It is difficult to distinguish between IPSA1 and IPSA3 from these plots. The plots show that EDT is not a good choice due to low target coverage, and IPSA2 is not a good choice due to too high doses to OARs.

Summary Since tolerance limit to one or more OARs has been exceeded for 82% of the treatment plans for IPSA2, this procedure should be rejeceted. The target coverage is better, but reduction of dose is necessary due to the OARs, which then will result in loss of target coverage.

The results for IPSA3 was as expected. Inhomogeneity in dwell times were

reduced using this plan, but loss of target coverage then occurred. It is difficult to distinguish between IPSA1 and IPSA3, one having the better target coverage, the other sparing surrounding tissue more. Due to the reduction in high dose areas, IPSA3 will be preferable.

EDT is not a good suggestion. Little normal tissue is irradiated and the distribution of dwell times is homogeneous, but target coverage is poor. IPSA3 is better regarding the OAR, indicating that adapting the dose distribution to the patient's individual anatomy is useful. Manual alteration will be necessary for many EDT treatment plans. Still, EDT is an option available in Masterplan. An extra licence needs to be purchased to be able to use IPSA.

5.4 Exclusion of non-tissue material

Non-tissue material (applicator and vaginal packing) constitute a considerable part of the volume irradiated in brachytherapy of cervical cancer. When for instance evaluating volume receiving the prescribed dose, it is important to know if this volume includes or excludes the non-tissue material. In table 8 values have been calculated, when including and excluding the non-tissue material.

The treatment plans would be rated the same way, since IPSA2 $\geq$ IPSA1 $\geq$ IPSA3 $\geq$ EDT for both values that includes or excludes non-tissue material.

As expected, all dose and volume values where the non-tissue material is included is greater than the values where non-tissue material has been excluded, CTV V100 and CTV V400 having the largest differences. If these values were to be compared with other studies, data including this material would give false positives. For example, TC is higher when including the non-tissue material, since non-tissue material within CTV will most likely be fully covered, resulting in a false better target coverage. It is evident that full coverage of the applicator is irrelevant when it comes to the quality of the treatment.

High dose areas, even if situated within CTV, is unwanted since the clinical consequence is unknown. From the table, a substantial amount(approximately one half) of the regions receiving 400% of the prescribed dose is within the applicator, and from this it is evident that not excluding the non-tissue material will give misleading results, and the non-tissue volume should be excluded to get more correct results. Non-tissue material was manually delineated and subtracted from the parameters in this study. There exist a modality with predefined applicators with information on applicator volume, such that exclutions of applicator material can be done automatically.

As previously stated, when comparing treatment plans with each other irradiated non-tissue material will not alter the conclusions, but if the actual measure of the values were to be considered, non-tissue material should be excluded in order to get more reliable numbers.

5.5 Further study

Differences in mean values of dose and volume parameters between the different treatment plans are not statistically significant for all values evaluated here. However, using these numbers together with the plots and dose to the OAR, a tendency is found. Gathering more information would have been informative.

Target optimization will be avaible in Masterplan for the customers in June 2009. This may be a better alternative than EDT, but does not take OARs into consideration. It would have been interesting to assess this algorithm and compare it to IPSA1 and IPSA3. It is assumed that IPSA will give a better treatment plan, but the effect of this is not known.

Instead of searching for one set of dose constraints adequate for all cervical cancer patients, it might be possible to obtain several sets of different dose constraints. Which set to use could result from a parameter, e.g. there could be different sets of dose constraints for different width of target volumes. The plan created by IPSA might then be more adequate for the patient.

6 Conclusion

By comparing the dose distributions calculated by Masterplan and Plato, deviations was found in certain regions. When these regions were examined more carefully, they were found to be of no clinical relevance for brachytherapy for cervical cancer and these deviations are therefore not important. In clinically relevant areas, dose distributions calculated by Masterplan and Plato were similar. The two computer programs simulates the dose distribution for the two different sources that were to be compared, and therefore the dose distribution for the source types themself should be similar in clinical relevant areas. Simulating the GammaMed source used for treatment at St. Olavs Hospital by the Nucletron source available in Masterplan should be feasible. Dose measurements support this statement.

Treatment plans with different dose constraints created by the IPSA algorithm have been evaluated in this study. In addition to target coverage, sparing OARs and high dose areas have been of particular interest. One IPSA optimized treatment plan was found to give adequate dose distribution on average and is considered to be a better starting point for at treatment plan than the other suggestions. This plan included a constraint diminishing high dose areas and conservative constraints to OARs in addition to dose constraints for target coverage.

The IPSA plans were compared to a conservative treatment plan with equal dwell times where the dose was prescribed to the target surface. This plan will result in a poor starting point when creating a treatment plan in contrast with the IPSA optimized treatment plans.

A A calculation example of accumulated charge to dose rate in water

Parameters:

Calibration date for the source	15.12.2008	
Date of measurements	19.03.2009	
Days since calibration	94.5	d
Half life of ^{192}Ir	73.831	d
Decay factor from table	2.43	
Pressure, P	103.58	kPa
Temperature, T	21.3	°C
Accumulation time, t	60	s
Calibration factor for air-kerma rate, N_k	$43.8 \cdot 10^6$	Gy/C
Average of accumulated charge	**1.159**	nC
Noise	5.3	pC
Average of accumulated charge, corrected	**1.154**	nC

By using equation (3) in section 2.2.4, the correction factor for pressure and temperature is

$$k_{TP} = \frac{(273.2 + 21.3)}{(273.2 + 20)} \cdot \frac{101.3}{103.58} = 0.982$$

The decay factor can be calculated from equation (5).

$$\frac{1}{F_{decay}} = \frac{1}{e^{-ln2 \cdot 94.5/73.83}} = 2.43$$

This is the same as the decay factor from the table. Thus, from equation (4) and (5) the dose rate is found.

$$\dot{D}_{W,Q} = \frac{1.1537 \cdot 10^{-9}}{60/3600} \cdot 43.8 \cdot 10^6 \cdot 1.11 \cdot 1 \cdot 0.982 \cdot 1 \cdot 1 \cdot 2.43 = 8.03 Gy/h.$$

B Calculation of tolerance limit per fraction for OARs

To calculate the total biological weighted dose from both external and internal radiation therapy, each fraction of external and internal radiotherapy has to be evaluated, and a biologically weighted dose (doses relative to 2 Gy fractions, with the same α/β-value) has to be calculated. These calculated values from each fraction can be added, arriving at the total biologically dose that was given to the volume of interest.

The maximum dose, d, an OAR can receive in each of the four fractions of brachytherapy can be found as shown in the following.

Parameters:

Number of brachytherapy fractions	4	
Dose to CTV per brachytherapy fraction	5	Gy
α/β-value for normal tissue	3	
α/β-value for tumor tissue	10	
Tolerance limit for bladder	90	Gy
Tolerance limit for rectum and sigmoid	75	Gy
Total dose from external treatment (25 fractions)	50	Gy

The tolerance limit per fraction for the bladder can then be calculated from equation (1) :

$$\begin{aligned} EQD_2(internal) = 90\ Gy - 50\ Gy &= 40\ Gy \\ EQD_2 = 4d \cdot \frac{d+3}{2+3} &= 40\ Gy \\ d^2 + 3d &= 50 \\ d &= 5.7 \end{aligned}$$

The minimum dose in the 2 cm^2 volume that receives the highest dose should therefore not be greater than 5.7 Gy per fraction for the bladder. To be conservative, a worst case scenario is considered, i.e. it is assumed that the highest dose will occur in the same part of the organ for every fraction.

C Data file from comparison of dose calculated by Masterplan and Plato

The data file for the plots in figure 22 and 23 in chapter 4.1 are given in table 9. Absolute values of the difference between point doses calculated by Masterplan and Plato are given in percentages of the point dose calculated by Plato.

Table 9: *Deviations for given points in calculated dose by Masterplan and Plato*

Point source			*Catheter*		
x	z	*Deviation (%)*	x	z	*Deviation (%)*
5	25	0.77	1	1.7	2.5
10	25	0.34	2	3.5	2.7
15	25	0.2	4	6.9	0.5
20	25	0.31	8	13.8	0.2
25	25	0.53	16	27.6	0.2
30	25	0	0.5	1.9	15.8
5	0	0.55	1	3.9	6.6
10	0	0.22	2	7.7	1.7
15	0	0.16	4	15.4	0.3
20	0	0.17	8	30.8	0
25	0	0.32	16	61.6	0.2
30	0	0.3	0.5	3	11.1
0	2	126.3	1	6	0.2
0	4	19.5	1.3	7.8	3
0	6	7.8	2	12	0.2
0	7	5.1	4	24	0.6
0	8	3.4	0.3	3.3	24.2
0	10	3.2	0.5	5.5	11.9
0	12	3.1	0.7	8	8.7
0	14	3	1	11	0.1
0	16	2.9	5	55	1.9
0	18	2.7	1	-1.7	10.8
0	20	2.6	1.5	-2.6	8
0	22	2.2	2	-3.5	5.7
0	24	1.8	3	-5.2	3.7
0	26	2	4	-6.9	2.9
0	28	2.7	8	-13.8	1.9
0	30	3.6	16	-27.6	2.2

Point source			*Catheter*		
x	y	*Deviation (%)*	x	y	*Deviation (%)*
0	35	0	0.5	-1.9	18.7
0	40	1.1	0.7	-2.9	9.1
0	60	2.1	1	-3.9	5.5
2	20	1.8	0.7	-4.5	4.8
4	2	1.6	1	-6	3
4	4	2.5	1.3	-7.8	1.7
4	6	1.8	2	-12	0.6
4	8	1.5	0.3	-3.3	1.8
4	10	1.8	0.5	-5.5	0.8
4	20	1.4	0.7	-8	3.2
0	-2	16.1	1	-11	6.7
0	-4	9.4	2	-22	5.9
0	-6	8	1	51.7	6.1
0	-8	6.9	2	53.5	4.3
0	-10	7.3	4	56.9	1.7
0	-12	12.4	8	63.8	0.7
0	-14	19.4	16	77.6	1.3
0	-16	27.4	0.5	51.9	21.5
0	-18	36.3	1	53.9	6.7
0	-20	45.9	1.5	55.8	3.1
0	-22	41.7	2	57.7	2
0	-24	37.3	4	65.4	1.1
0	-26	34.6	8	80.8	1.7
0	-28	33.5	0.5	53	13.5
0	-30	32.2	0.7	54.4	5.8
0	-35	28.2	1	56	3
0	-40	27.2	1.3	57.8	2
0	-60	13.8	2	62	2
0	-80	13.1	0.3	53.3	14.9
2	-2	7	0.4	54.4	7.3
2	-4	7.5	0.5	55.5	3.5
2	-8	5.4	0.7	58	1.6
2	-12	3.8	1	61	2.3
2	-16	2	1	48.3	6.2
2	-20	0.5	2	46.5	0.7
2	-24	2.7	4	43.1	0.1
2	-28	6	8	36.2	0.1
2	-32	7.4	16	22.4	0.1
2	-36	8	0.5	48.1	12.4
2	-40	9.5	1	46.1	0.8
2	-44	13.2	2	42.3	0.5
2	-48	15.7	4	34.6	0.3

Point source			*Catheter*		
x	*y*	*Deviation (%)*	*x*	*y*	*Deviation (%)*
2	-52	14.8	8	19.2	0.1
2	-56	10.8	0.5	47	16.6
2	-60	6.1	1	44	5.4
2	-64	3.9	1.3	42.2	0.3
2	-68	3.3	2	38	1.9
4	-2	2.6	0.3	46.7	21
4	-4	3.3	0.5	44.5	21.2
4	-8	4.1	0.7	42	6.8
4	-12	2.5	1	39	5.5
4	-16	2.3	0	-2	14.8
4	-20	2.6	0	-4	11.7
4	-24	2.7	0	-6	13.5
4	-28	1.4	0	-8	16.3
4	-32	0.7	0	-10	19.9
4	-36	0.5	0	-12	24.5
4	-40	0.2	0	-14	28.9
4	-44	0.6	0	-16	31.6
4	-48	1.8	0	-18	33
4	-52	2.4	0	-20	34
4	-56	1.7	0	-22	31.9
4	-60	0.1	0	-24	29.9
4	-64	0.9	0	-26	28.5
4	-68	1.6	0	-28	27.4
1	1.7	5.07	0	-30	26.5
2	3.5	4.46	0	-60	8.6
4	6.9	0.75	0	-90	3
8	13.8	1.13	2	-2	6.1
16	27.6	0.08	2	-4	5.8
0.5	1.9	20.52	2	-8	2.2
1	3.9	7.79	2	-12	0.6
2	7.7	1.64	2	-16	3.2
4	15.4	2.2	2	-20	5.4
8	30.8	0.12	2	-24	7.3
0.5	3	15.28	2	-28	8.6
1	6	3.16	2	-32	9.1
1.3	7.8	1.42	2	-36	9.3
2	12	2.67	2	-40	9.5
3	18	0.21	2	-44	8.8
4	24	0.9	2	-48	7.6
0.3	3.3	17.61	2	-52	5.9
0.5	5.5	4.29	2	-56	4.3
0.7	8	1.03	2	-60	2.6

Point source			*Catheter*		
x	y	*Deviation (%)*	x	y	*Deviation (%)*
1	11	2.95	2	-64	1.6
1.5	16.5	0.35	2	-68	0.4
2	22	1.46	4	-2	2.6
1	-1.7	11.63	4	-4	2.8
2	-3.5	7.09	4	-8	2.7
4	-6.9	4.25	4	-12	1.6
6	-10.4	2.58	4	-16	1.3
8	-13.8	1.77	4	-20	1
16	-27.6	2.04	4	-24	0.5
0.5	-1.9	19.83	4	-28	0
1	-3.9	7.86	4	-32	0.3
2	-7.7	5.54	4	-36	0.3
3	-11.6	3.4	4	-40	0.4
4	-15.4	2.41	4	-44	0
8	-30.8	2.36	4	-48	0.5
0.5	-3	10.82	4	-52	1.1
1	-6	8.32	4	-56	2.1
1.3	-7.8	7.64	4	-60	2.7
1.7	-10.2	4.8	4	-64	3.4
2	-12	3.8	4	-68	4.2
3	-18	0.27	0	52	123.7
4	-24	0.27	0	53	27.8
0.3	-3.3	4.39	0	54	15.7
0.5	-5.5	7.4	0	55	9
0.7	-8	5.67	0	56	6
0.8	-9	3.6	0	57	4.2
1	-11	1.5	0	58	3.1
1.5	-16.5	0.12	0	60	2.8
2	-22	1.11	0	62	2.6
			0	64	2.3
			0	66	2
			0	68	1.7
			0	70	1.4
			0	72	1
			0	74	0.7
			0	76	0.4
			0	78	0.1
			0	80	0.2
			0	90	2.5
			2	52	3.9
			2	54	4
			2	56	2.7

Point source			*Catheter*		
x	y	*Deviation (%)*	x	y	*Deviation (%)*
			2	58	2
			2	60	2.1
			4	52	2
			4	54	2.5
			4	56	1.9
			4	58	1.6
			4	60	1.6
			5	25	0.1
			10	25	0
			15	25	0.2
			20	25	0.1
			25	25	0.1
			30	25	0.2

D P-values for the difference in means

The P-values (6 pairwise comparisons) calculated for the difference in mean values for dose and volume parameters from the four treatment plans in table 5 in chapter 4.3. The P-value is outlined for the values where the difference is significant.

CTV D90	*EDT*	*IPSA1*	*IPSA2*	*IPSA3*
IPSA1	**0.0004**		0.2	0.6
IPSA2	**0**			**0.009**
IPSA3	**0.01**			

CTV V100	*EDT*	*IPSA1*	*IPSA2*	*IPSA3*
IPSA1	0.5		0.9	1.0
IPSA2	0.2			0.8
IPSA3	0.7			

CTV V400	*EDT*	*IPSA1*	*IPSA2*	*IPSA3*
IPSA1	0.8		0.9	0.8
IPSA2	0.4			0.4
IPSA3	1			

EXT V100	*EDT*	*IPSA1*	*IPSA2*	*IPSA3*
IPSA1	**0.002**		0.2	0.6
IPSA2	**0**			**0.01**
IPSA3	0.054			

Bladder	*EDT*	*IPSA1*	*IPSA2*	*IPSA3*
IPSA1	0.9		0.4	0.6
IPSA2	0.1			**0.041**
IPSA3	1.0			

Rectum	*EDT*	*IPSA1*	*IPSA2*	*IPSA3*
IPSA1	0.058		0.7	0.9
IPSA2	**0.003**			0.3
IPSA3	0.2			

Sigmoid	*EDT*	*IPSA1*	*IPSA2*	*IPSA3*
IPSA1	0.08		0.4	1.0
IPSA2	**0.001**			0.2
IPSA3	0.2			

TC	*EDT*	*IPSA1*	*IPSA2*	*IPSA3*
IPSA1	**0**		0.1	0.9
IPSA2	**0**			**0.02**
IPSA3	**0.0004**			

COIN	*EDT*	*IPSA1*	*IPSA2*	*IPSA3*
IPSA1	0.3		1.0	0.9
IPSA2	0.2			0.9
IPSA3	0.08			

COIN weight	*EDT*	*IPSA1*	*IPSA2*	*IPSA3*
IPSA1	**0.001**		0.5	1.0
IPSA2	**0**			0.4
IPSA3	**0.002**			

E Plots of COIN(weight) vs. OAR

The plots for COIN(weight) versus rectum and sigmoid used to count the total number of plans positioned in upper left square in table 6 are shown in figure 33 and figure 34.

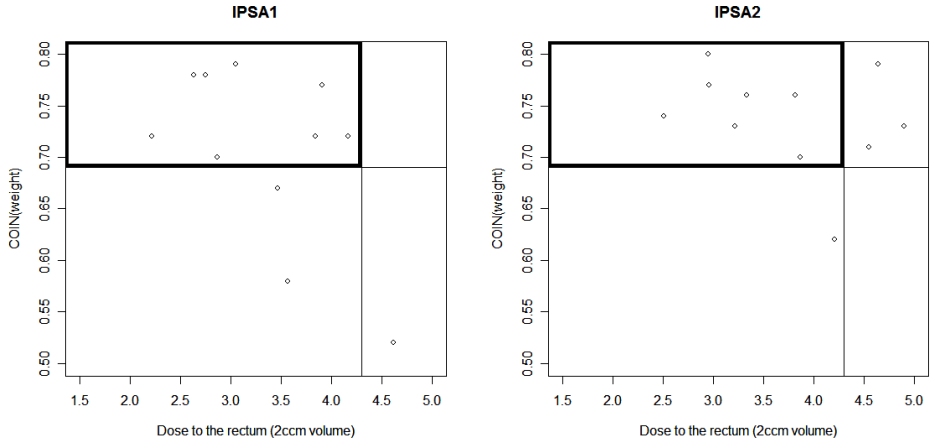

(a) IPSA1

(b) IPSA2

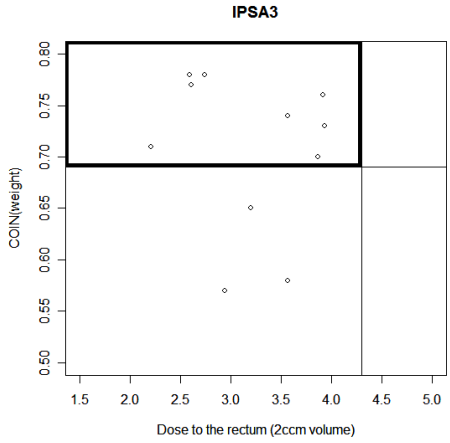

(c) IPSA3

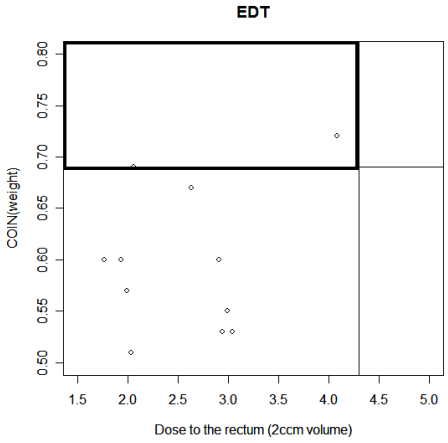

(d) EDT

Figure 33: *COIN(weight) vs. minimum dose in the volume* ($2\ \mathrm{cm}^3$) *receiving the highest dose for the rectum. Points in the upper left square fulfill the constraints with respect to the* OAR *and* COIN*(weight) is better than average.*

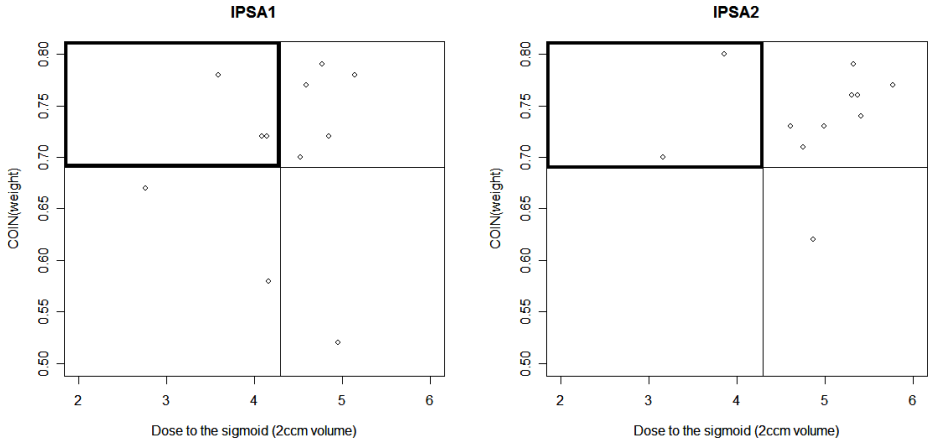

(a) IPSA1

(b) IPSA2

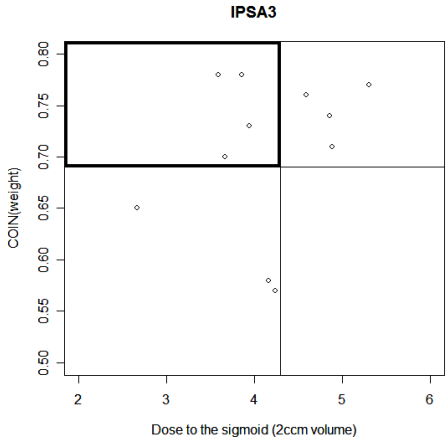

(c) IPSA3

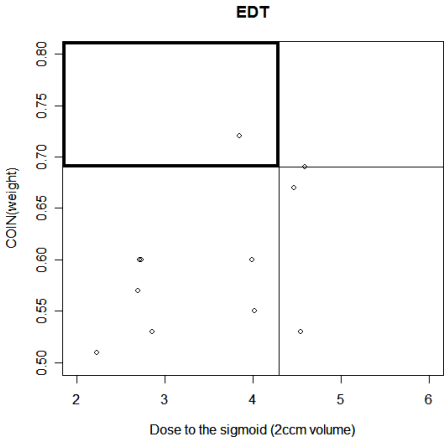

(d) EDT

Figure 34: *COIN(weight) vs. minimum dose in the volume* ($2\ \mathrm{cm}^3$) *receiving the highest dose for the sigmoid. Points in the upper left square fulfill the constraints with respect to the* OAR *and* COIN*(weight) is better than average.*

References

[1] Ingrid Langdal. 3D individual treatment planning compared with standard planning in intracavitary radiation therapy of cervix cancer. Project work, Norwegian University of Science and Technology, 2008.

[2] Oncolex. `http://www.oncolex.no/Livmorhals.aspx`. (downloaded 10.05.09).

[3] Gerbaulet A, Pötter R, Mazeron J, Meertens H, and Van Limbergen E. *The GEC ESTRO handbook of Brachytherapy*. 2002.

[4] Haie-Meder C and Pötter R et al. Recommendations from Gynaecological (GYN) GEC ESTRO working group (i): Concepts and terms in 3D image-based 3D treatment planning in cervix cancer brachytherapy with emphasis on MRI assessment of GTV and CTV. *Radiotherapy and Oncology*, (74):235–245, 2005.

[5] DeWitt K, Hsu C J, and Speight J et al. 3D inverse treatment planning for the tandem and ovoid applicator in cervical cancer. *International Journal of Radiation Oncology Biology and Physics*, 63(4):1270–1274, 2005.

[6] Venselaar J and Pérez-Calatayud J. *A practical guide to quality control of brachytherapy equipment*. 2004.

[7] Waggoner S E. Cervical cancer. *Lancet*, (361):2217–25, 2003.

[8] Veileder i gynekologisk onkologi. 2002.

[9] International commission on radiation units and measurements. *Prescribing, recording and reporting photon beam therapy (supplement to ICRU report 50)*. 1999.

[10] Varian. Varian brachytherapy applicator catalouge. `http://www.varian.com/media/oncology/brachytherapy/pdf/VBT\_Applicator\_Catalogue.pdf`. (downloaded 05.06.09).

[11] Stone H, Coleman N, Anscher M, and McBride W. Effects of radiation on normal tissue; consequences and mechanisms. *Lancet Oncology*, (4, 529-536), 2003.

[12] Hall E and Giaccia A. *Radiobiology for the radiobiologist*. 2006.

[13] Pötter R, Haie-Meder C, Limbergen E, and Barillot I. Recommendations from gynaecological (GYN) GEC ESTRO working group (ii): Concepts and terms in 3D image-based treatment planning in cervix cancer brachytherapy - 3D dose volume parameters and aspects of 3D image-based anatomy, radiation physics, radiobiology. *Radiotherapy and Oncology*, 78(78):67–77, 2006.

[14] Coursebook:. *ESTRO teaching course on brachytherapy in gynaecological malignancies.* 2006, 31.08-02.09.

[15] Steel G. G. *Basic clinical radiobiology.* 2002.

[16] Ballester F, Puchades V, and Lluch J et al. Technical note: Monte-Carlo dosimetry of the HDR 12i and Plus ^{192}Ir sources. *Medical Physics*, 28(12):2586–2591, 2001.

[17] Williamson J F and Li Z. Monte Carlo aided dosimetry of the microselectron pulsed and high dose-rate ^{192}Ir sources. *Medical Physics*, 22(6):809–818, 1995.

[18] Mayles P, Nahum A, and Rosenwald J-C. *Handbook of radiotherapy physics.* 2007.

[19] IAEA TECDOC 1247. *Calibration of photon and beta ray sources used in brachytherapy.* 2002.

[20] Nath R, Anderson L, and Luxton G et al. Dosimetry of interstitial brachytherapy sources: Recommendations of the AAPM Radiation Therapy Committee Task Group No. 43. *Medical Physics*, 22(2):209–234, 1995.

[21] American Association of Physicists in Medicine AAPM. Specification of Brachytherapy source strength. *Report 21 of Radiation Therapy Committee Task Group 32*, 1987.

[22] Nucletron. `http://www.nucletron.com`. (downloaded 06.06.09).

[23] Kirkpatrick S. Optimization by simulated annealing: Quantitative studies. *Journal of Statistical Physics*, 34:975–986, 1983.

[24] Nucletron. User manual: Oncentra Masterplan, Physics and Algorithms.

[25] Lomax N and Scheib S. Quantifying the degree of conformity in radiosurgery treatment planning. *International Journal of Radiation Oncology Biology and Physics*, (55):1409–19, 2003.

[26] Baltas D, Kolotas C, and Geramani K et al. A conformal index (COIN) to evaluate implant quality and dose specification in brachytherapy. *International Journal of Radiation Oncology Biology and Physics*, 40(2):515–524, 1998.

[27] Oozeer R, Chauvet B, and Garcia R et al. Évalution dosimetrique d'une radiothérapie conformationnelle: le facteur de conformation. *Cancer Radiotherapy*, (4):207–216, 2000.

[28] Box G, Hunter W, and Hunter J. *An Introduction to Design, Data Analysis and Model Building.* 1978.

[29] Department of Statistics and Mathematics of the WU Wien. http://www.r-project.org/. (downloaded 11.06.09).

[30] EMBRACE. https://www.embracestudy.dk/. (downloaded 08.06.09).

[31] Kubicky C, Yeh B, and Lessard E et al. Inverse planning simulated annealing for magnetic resonance imaging-based intracavitary high-dose-rate brachytherapy for cervical cancer. *Brachytherapy*, 7:242–247, 2008.

[32] Chajon E, Dumas I, and Touleimat M et al. Inverse planning approach for 3-D MRI-based pulse-dose rate intracavitary brachytherapy in cervix cancer. *International Journal of Radiation Oncology Biology and Physics*, 69(3, 955-961), 2007.

[33] π medical research. http://www.pi-medical.gr/development/hipo. (downloaded 13.06.09).